RICE UNIVERSITY

Change in Cell Motility and Metabolism Following Culture under Low Shear Conditions

by

Sean Patrick Lennon

A THESIS SUBMITTED
IN PARTIAL FULFILLMENT OF THE
REQUIREMENTS FOR THE DEGREE

Master of Science

APPROVED, THESIS COMMITTEE:

Kyriacos Zygourakis, A.J. Hartsook Professor and Chair, Chemical & Biomolecular Engineering

Nikos V. Mantzaris, Associate Professor, Chemical & Biomolecular Engineering

Kevin R. MacKenzie, Assistant Professor, Biochemistry and Cell Biology

HOUSTON, TX
DECEMBER 2007

ABSTRACT

^{1}H-NMR Investigation of Enhanced Migratory Behavior of

Lymphocytes Cultured in a Rotating Wall Vessel

By

Sean Patrick Lennon

Recent studies suggest that the human immune system, and in particular lymphocyte function, may be suppressed during space flight. However, the mechanisms by which mechanical forces affect the function of immune cells are still poorly understood. Research performed in our laboratory indicates that culturing lymphocytes under low shear conditions (in rotating wall vessels) leads to an increase in cell motility and altered cell morphology. We have hypothesized that fundamental changes in the cytoskeleton, caused by changes in external forces, could lead to secondary changes in cellular metabolism, which could in turn be reflected by altered membrane structure. Utilizing NMR to investigate changes in lymphocyte function in an altered mechanical environment, we observed significant changes in cell metabolism following cell culture in the RWV, as compared to cells cultured statically. Our research seeks to advance the understanding of how microgravity affects the function of individual cells and how these cells interact with their environment.

Acknowledgements

I would like to express my sincere appreciation to my thesis committee: Dr. Kyriacos Zygourakis (Advisor), Dr. Nikos Mantzaris and Dr. Kevin MacKenzie. Thank you for your time, assistance, and above all, patience. This thesis has taken an unusual path and I appreciate you understanding and commitment along the way. I would like to genuinely thank Sean Moran for his assistance with the NMR experiments. Sean dedicated many afternoons with me to help me stick to my experimental schedule. Finally, I would like to thank Dr. Jan Post for introducing me to the science of NMR and its potential in the field of Bioengineering and Cell Biology.

Table of Contents

Table of Figures

1. INTRODUCTION

1.1. Overview

Several studies have suggested that the human immune system, and in particular lymphocyte function, may be suppressed during space flight [17, 19, 20]. This is possibly caused by microgravity-induced physiological changes – such as fluid redistribution and cardiovascular deconditioning - that can alter the mechanical force environment of lymphocytes. However, the mechanisms by which mechanical forces affect the function of immune cells are still poorly understood.

Research performed in our laboratory indicates that culturing lymphocytes under low shear conditions (in rotating wall vessels) leads to an increase in cell motility and altered cell morphology. As has been observed with malignant cells, motility changes may be modulated by prolonged stimulation of protein kinase C (PKC) occurring via phosphatidylcholine (PC) cycles (Figure 1.1) that generate second messengers such as diacylglycerol (DAG). We have hypothesized that fundamental changes in the cytoskeleton, caused by changes in external forces, could lead to secondary changes in cellular metabolism, which could in turn be reflected by altered membrane structure.

Several studies have reported the appearance of narrow mobile lipid (ML) signals in ^{1}H NMR spectra in cells induced to apoptosis by exposure to antitumor drugs as well as activated lymphocytes and lymphoblasts [46,87]. These results raise the possibility that a common "activation" pathway exists for malignant cells and lymphocytes

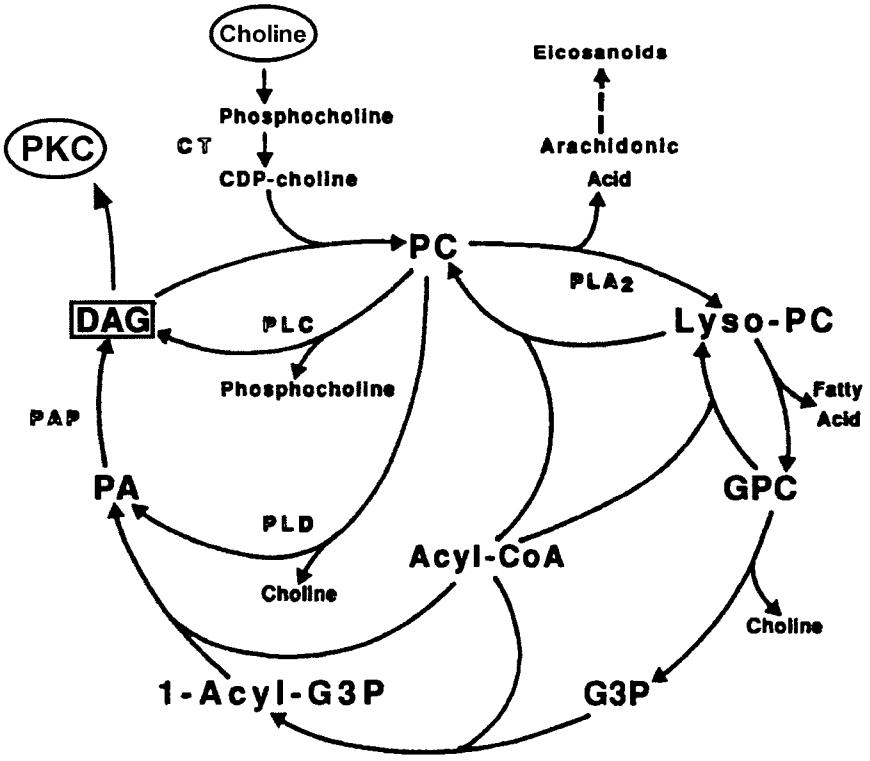

Figure 1-1: Phosphatidylcholine Cycle.

activated by either chemical stimuli or mechanical forces. Notably, both malignant cells and lymphocytes have the ability to migrate and thus elevated levels of ML may be associated with an increase in cell motility. The level of mobile lipid may correlate with the ability of malignant cancer cells to metastasize and the capacity of T-lymphocytes to migrate to the site of infection.

Furthermore, there is emerging evidence that the structural changes in the cytoskeleton (membrane fluidity) may play an important role in modulating the activity of PKC [44,51,52]. In fact, since the structure and function of membrane proteins depends on the lipid environment any perturbation of the cytoskeleton inevitably affects PKC activity.

1.2. Lymphocyte Adhesion and Migration

1.2.1. Role of Lymphocytes in the Immune System

Lymphocytes play a critical role in many aspects of the immune system. They produce antibodies that attack foreign pathogens (B cells), secrete cytokines that elicit immune responses from both the humoral and cell-mediated immune systems (T helper cells) and kill infected cells (cytotoxic T cells). B cell activation requires binding of free foreign antigen in the body, whereas T cell activation is induced through interactions with antigen presenting cells that display foreign antigen on their surface. Antigen presenting cells are specialized cells that ingest foreign pathogens by phagocytosis and display small sequences of pathogen proteins on its surface through major histocompatibility complex receptors. Thus, T cell function requires a specific sequence of immunological events and specific cell-cell interactions [1].

To effectively carry out immune functions, lymphocytes recirculate through the body, spending much of their time in the blood stream and lymphatic tissues. During the recirculation process, lymphocytes extravasate through the endothelium into the periphery. From there, they migrate either to a site of infection or to lymphatic ducts where they are transported to lymph nodes. From the lymph nodes, lymphocytes reenter the blood stream to start the recirculation process once again. Throughout this process, the interaction of lymphocytes with extracellular matrix proteins is critical in order to effectively recirculate or migrate to the site of infection. [1-4]

1.2.2. Cell Signaling

Protein kinase C (PKC) is a family of serine / threonine kinases that plays a critical role in many aspects of lymphocyte function. Upon activation of lymphocytes through the T cell receptor (TCR), PKC is activated as part of the signal transduction pathway involved in the immunological response [5]. PKC is also activated through the integrin signaling pathway [ibid]. Further, PKC is believed to have a pivotal role in the activation of FAK [ibid], which can activate the MAP kinase pathway and lead to changes in cell behavior [6, 7]. Without necessary co-stimulatory events from integrin binding, T cell activation can be inhibited [8]. One complication when considering PKC functions in cells is that several isoforms of the molecule exist with different biological functions that may be cell type specific [9]. The functions of each of these isoforms have not been sufficiently elucidated to determine the isoforms important in lymphocyte signaling. PKC can be stimulated directly using phorbol esters or inhibited using any number of PKC inhibitors. Experiments using these chemicals suggest that PKC

stimulation may lead to divergent cellular consequences depending on cell type and co-stimulatory factors [9, 10].

Clearly, PKC could play critical roles in modulating events necessary for cell migration and the integrated effects of these pathways may ultimately determine cell adhesion and migratory characteristics. Lymphocytes clearly can be affected by PKC stimulation upon activation and / or integrin binding, but the role of FAK is not yet clearly defined for this cell type. In the next section, the effects of modulating these pathways using inhibitors and stimulators of PKC and related signaling molecules on lymphocyte migration are presented and discussed.

1.2.3. Lymphocyte Migration: Role of Intracellular Signaling

Lymphocyte migration is modulated not only by cell-substrate interactions, but also by intracellular signaling pathways. It is believed that at least two separate pathways can modulate lymphocyte migration: the protein kinase C (PKC) pathway and the protein tryrosine kinase (PTK) pathway [11]. Both these pathways are involved in integrin signaling events. Moreover, PKC is a critical signaling molecule in the lymphocyte activation signaling pathway through the T cell receptor. Thus, one way that lymphocytes can modulate their adhesion and migration behavior upon activation is through the PKC pathway. Studies that have investigated the role of PKC in lymphocyte migration are discussed below.

Entschladen and coworkers treated unactivated peripheral lymphocytes with phorbol 12-myristate 13-acetate (PMA), a common agent used to stimulate the PKC pathway, and counted the number of motile cells in a collagen gel [11]. PMA significantly increased the percentage of motile cells, while PKC inhibitors did not affect

the percentage of migratory cells in the collagen gels (in the absence of PMA) [11]. These researchers believed that although PKC was inhibited, cell migration was still occurring in the cells due to the PTK pathway. Inhibition of the PTK pathway using genistein resulted in a reduction of the percentage of motile cells in the population. These experiments suggest that PMA enhances migration of lymphocyte in collagen gels, while PTK inhibitors inhibit lymphocyte migration [11].

However, other studies have been presented that are apparently not consistent with these findings. Researchers have reported that PKC inhibitors induce lymphocyte locomotion and PMA inhibits migration and cell polarization on a 2-D surface [12]. Furthermore, these researchers found that PKC inhibitors induced spontaneous lymphocyte invasion into collagen gels compared to untreated controls. Although lymphocyte migration was not assayed on the 2-D surface (both Molt-4 cells and unactivated peripheral lymphocytes were used for this study), the cells that were more polarized were believed to be more motile than non-polarized cells. These experiments suggest that PKC stimulation with PMA may inhibit cell migration [12].

Activation of lymphocytes using antibodies to CD2 and CD3 (the T cell receptor) also stimulates PKC and a change in lymphocyte migratory behavior. Recent studies reported that CD3 stimulation with an antibody enhances lymphocyte migration [13]. Activation via the CD3 antibody stimulates PKC in a different way than PMA. Integrin ligation and CD3 activation synergistically induces focal adhesion kinase phosphorylation and increases cell migration in 3-D collagen matrices [14]. Although PMA clearly stimulates PKC and affects lymphocyte migration, PMA does not induce focal adhesion kinase phosphorylation [14]. From these experiments, it appears that

PMA induces PKC activation differently than lymphocyte activation. One possible reason for this is that PMA and CD3 antibody activation could stimulate different isoforms (similar molecules with biologically distinct functions) of the PKC molecule.

Clearly, PKC activity in the cell affects lymphocyte migration, but the specific experimental materials, cells and methods used can result in apparently conflicting results. Since PMA has been shown to increase cell-ECM adhesiveness [15, 16], one possible mechanism by which PMA treatment could affect cell migration is by altering cell-substrate adhesiveness. Since PKC can phosphorylate proteins associated with the cytoskeleton, migration may also be affected by modulating cytoskeletal behavior.

1.3. Effects of Space flight on the Immune System

Space travel exposes the human body to a very different environment from that on Earth. As we plan for longer trips into space, we need to learn more about how the body reacts to the space environment so that we can anticipate health problems, both during flight and upon return to Earth. The fact that the bodies of astronauts change in many ways during flight has been known since the early days of space travel. Bones and muscles diminish, the immune system weakens, and the cardiovascular system alters to accommodate movement and the headward fluid shift that occurs in a weightless environment. Exposure to high levels of radiation also contributes to the potential adverse effects of space flight. In this section, a brief overview is presented of studies involving the effects of space travel, and in particular microgravity, on the immune system.

1.3.1. Depressed Immune System Function During Space Flight

Many studies have been carried out to elucidate the effect of space travel on the human immune system. These experiments can loosely be classified in three groups: *in vivo, ex vivo* and *in vitro* experiments. Direct measurements of immune function on human subjects assaying for an immune response to an antigen constitute the *in vivo* approach. *Ex vivo* experiments are carried out by removing immune cells from human subjects before, during and after space flight and assaying cell number or function. *In vitro* experiments consist of studies that compare immune cell function (in cell culture) in space versus ground-based experiments or an appropriate in-flight control. Although the results of many of the studies discussed below suggest there are changes in the immune system function in space, clinical cases have not yet been cited where depressed immune system function specifically associated with space travel has resulted in illness [17].

The most common *in vivo* experiment used on space travelers is the coetaneous delayed-type hypersensitivity response to recall antigens. This experiment, which measures the cell-mediated immune mechanism, involves injection of a small amount of antigen just under the skin and evaluating the immune response by measuring the amount of skin induration using a caliper. After injection, the antigen is taken up by an antigen-presenting cell and displayed on its surface. Then, lymphocytes interact with the antigen-presenting cell and elicit a localized immune response. Thus, the delayed-type hypersensitivity test has been established as a clinical test for T lymphocyte function [18].

Space shuttle astronauts showed a blunting of delayed-type hypersensitivity cutaneous response after 4-10 days in flight. Both the number of reactions and the extent of reaction were reduced in astronauts compared to preflight control values [19]. Similar experiments were performed on cosmonauts on longer missions on board the space station MIR. The cosmonauts were tested after 59-155 days in orbit and the results obtained were compared to pre-flight and post-flight data. Eighty percent of the cosmonauts tested showed a blunted response to the delayed type hypersensitivity test during space travel compared to controls. Also, 60 percent of the cosmonauts had recovered to preflight levels within 9 days after landing [20].

Several *ex vivo* experiments were also conducted where blood samples were collected from astronauts before and after space flight and compared. In these experiments, the number and function of immune cells were assayed to quantify the effect of space flight on immune system function. The number of blood lymphocytes decreased in 77 percent of astronauts after space flight. Conversely, the number of neutrophils in the blood increased in 40 out of 41 subjects tested. Also, the number of blood eosinophils was decreased after space flight [21-23].

In addition to a decrease in the blood lymphocyte number of astronauts after space flight, the function of the lymphocytes was also impaired compared to pre-flight controls. Phytohemaglutinin was used to activate lymphocytes and cell proliferation was measured using ^{3}H-thymidine incorporation into the cellular DNA and RNA. (Phytohemaglutinin is an exogenous agent that activates resting lymphocytes into a lymphoblast, which then proliferates and synthesizes new DNA and RNA.) ^{3}H-thymidine incorporation was reduced in 36 of 41 subjects after flight, indicating a

reduced activation potential of lymphocytes after space travel [23]. Thus, lymphocyte number and function were both decreased in astronauts after space travel.

The amount of immunoglobulins and complement proteins found in the blood after space flight has also been studied. Significant changes in immunoglobulin levels were not detected [24, 25], except in long duration flights where the changes may be due to an immunological response to the degradation of skeletal tissues [25]. Experiments measuring the amount of complement components in the blood were inconclusive since a decrease, increase or no change was seen for different flights [24-27].

Immune cells isolated from rats after space travel were also altered compared to ground-based controls. Rat bone marrow and spleen cells were analyzed for important cell surface receptors using flow cytometry. A significant increase in interleukin-2 receptor expression was noted for splenic lymphocytes from rats that experienced space travel [26]. Bone marrow cells isolated from rats exposed to space travel also showed a significant increase in IgG immunoglobulin expression [26]. Splenic lymphocytes isolated from the rats also showed a depressed ability to produce interferon-γ (an important cytokine) in response to an activating factor (concanavalin-A) [27].

In conclusion, the studies discussed in this section have shown that the immune system is affected, and probably depressed during travel in space. In particular, lymphocyte number and function appear to be decreased in people and animals during space travel. However, the mechanism of how the immune system in depressed in space is poorly understood. The immune system is affected by many factors during space travel that may work together. These factors include physical and psychological stress, cosmic radiation, microgravity and changes in other physiological systems within the

body [17]. Certainly, stress without space travel has been shown to depress immune function [28]. To understand how microgravity may effect cellular, and in particular lymphocyte behavior, a discussion concerning behavior of cells cultured in space is now presented.

1.3.2. Effect of Microgravity on Cell Culture

Several *in vitro* studies have been reported that suggest gravity does indeed affect single cell behavior in culture. Lymphocytes were cultured in space, on the ground, or in an in-flight control centrifuge (used to apply a 1*g* force to the cells) and their behavior (activation efficiency and production of cytokines upon activation) was compared [29]. Since the cells can be exposed to extreme conditions during take-off and landing of the aircraft, the 1*g* control centrifuge is a key development in space experimentation that allows for the controls necessary for direct measurement of the effects of gravitational forces on cell behavior.

Isolated peripheral lymphocytes were cultured and activated with concanavalin A in space and compared to ground and flight centrifuge controls. ^{3}H-thymidine incorporation into the DNA and RNA was severely inhibited in cells cultured in microgravity compared to ground and in-flight controls, indicating a decreased activation potential of the cells [29]. Further, Jurkat cells (a T lymphoblastoid cell line) exposed to microgravity exhibited a decrease in production rate of cytokines (interleukin-1 and interleukin-2) upon activation with phorbol esters [30]. Additional studies showed that the production of interferon-γ by lymphocytes may be inhibited by microgravity [31]. Together, these studies indicate that microgravity might have a negative effect on the function of lymphocytes *in vitro*.

In contrast, lymphocyte activation and cytokine production was increased in microgravity for cells immobilized on Cytodex microcarrier beads [30]. ^{3}H-thymidine incorporation upon activation with concanavalin A was significantly increased in microgravity for cells attached to the solid substrate, while DNA synthesis was lower than controls for cells cultured in suspension (in agreement with cells cultured in suspension as discussed above). Further, interferon-γ production, which is severely inhibited in microgravity for lymphocytes cultured in suspension, was increased for cells cultured on the microcarrier beads in microgravity [30].

The studies discussed in this section showed that lymphocyte function is affected *in vitro* by microgravity. Lymphocytes cultured in suspension generally showed decreased immunological function in agreement with previously described *in vivo* and *ex vivo* studies that also showed depressed immunological function. Thus, these data support the idea that microgravity may inhibit immune cell function (since other factors associated with space flight such as cosmic radiation and stress are offset by the in-flight 1g centrifuge controls). Although it is clear that microgravity affects cellular and immune system function, the mechanisms through which reduced gravity influences cell behavior are unclear. In Section 1.4, the mechanisms concerning how microgravity may affect cells in the body are investigated.

1.3.3. Fluid Redistribution in Microgravity

Many physiological changes occur in the human body upon exposure to microgravity. One of these changes is fluid redistribution to the upper part of the body since gravity no longer pulls fluids toward the ground (and the lower portion of the body). This redistribution is sometimes manifested in astronauts as facial edema, nasal

congestion and headaches. Clearly, this phenomenon affects the cardiovascular system and could influence the function of associated cells and tissues such as lymphocytes and other immune cells. To characterize the effects of fluid redistribution on mammalian physiology, two ground-based methods have been used: (1) rat hind limb suspension and (2) human bed rest with a 6° head down tilt. Both methods result in fluid redistribution to the upper body and changes in cardiovascular physiology.

Rat hind limb suspension results in approximately a 10% increase in cardiac output [34]. Since fluid tends to be redistributed toward the heart and upper body, this is not an unexpected result. Humans exposed to the head down tilt exhibited significant differences in blood pressure and coetaneous blood flow rates. Mean arterial blood pressure increased only moderately (5%), but coetaneous blood flow showed large increases in both the cheek (150% of baseline) and the leg (400% of baseline) [32]. Other studies show that microgravity affects subcutaneous vascular resistance in humans [33].

These studies suggest that microgravity does influence fluid flow in the body in the heart, arteries and especially in peripheral tissues. These changes can certainly affect the mechanical forces acting on cells in the blood and tissues under microgravity conditions. It is our hypothesis that altered mechanical forces on cells and tissues may be a significant factor in depressed immune system function and as well as other physiological changes observed in space. To help confirm this hypothesis, we will subject immune cells (lymphocytes) to an altered mechanical environment utilizing a rotating wall vessel. Video microscopy and ^{1}H-NMR will be used to observe and

understand the functional and physiological changes caused by this altered mechanical environment.

1.4. Biological NMR Applications

Nuclear magnetic resonance (NMR) spectroscopy is a powerful technique that provides information on biochemical status and physiological processes of cells. NMR is a unique non-invasive research tool enabling the metabolism of intact cells and tissues to be studied in a continuous manner. In addition to intact tissues, NMR studies of metabolism can be performed with cellular extracts and cell suspensions. An area where NMR has been shown to help the study of metabolism is in the characterization of bioreactors and cell perfusion systems. Often, the only indicator of the cellular oxygen level is the difference between inflow and outflow oxygen partial pressure. With the recent development of a ^{19}F NMR technique, the oxygen partial pressure in gels used to entrap cells can be measured, which can accurately characterize the local oxygen environment around the cells [34].

The location and growth of cells in a hollow-fiber bioreactor can also be difficult to monitor. NMR imaging can provide non-invasive measure of the spatial variation of cells within the bioreactor [35]. Using diffusion weighted imaging, locations in the bioreactor that contain water with a large diffusion coefficient are assigned to extracellular water, whereas locations with a small diffusion coefficient are considered to be composed primarily of cells. In a similar study NMR microscopy was used to monitor the development of three-dimensional cartilage growth [36]. This technique allows for the evaluation of overall growth and localized intrinsic properties without disruption of the sample. NMR measurements are dependent on the chemical characteristics of the

tissue. Therefore evaluation of cell characteristics and extracellular matrix composition can be made independently. In another study, NMR microscopic methods were adopted to investigate the dynamics of prostate cancer cell invasion [37]. Measurements over several time points of the same sample reduce the variability introduced by using different sample preparations [38]. Proton spectroscopic imaging provides information about cell environment and metabolism in the cancer cells that is not available with conventional methods.

NMR studies of cells have achieved encouraging results in cancer research. Tumor cell metabolism is currently being examined to gain insight into the differences between normal and neoplastic tissues, to detect prognostic markers of malignancy, and to monitor the effect of therapies [39]. In recent years, attention has been focused on examining the proton NMR (^{1}H-NMR) spectra of tumor cells in culture. Tumor cells are characterized by narrow peaks from lipids, mostly triglycerides, clustered in mobile membrane domains. These signals have been shown to be present in a variety of cells [40-42]: in embryonic cells such as myoblasts [43]; in actively proliferating cells such as activated lymphocytes [44]; and in neutrophils [45], and B cells [46]. In some cases, malignant cells could be identified from normal cells on the basis of lipid signal intensity [47].

The nature of these membrane triglyceride signals remains unclear. The narrow ^{1}H-NMR peak widths from these molecules may be explained by a physicochemical model, which includes isotropic rotational diffusion, otherwise their ^{1}H-NMR spectra would consist of extremely broad and featureless resonances, typical of the restricted motion of membrane phospholipids [48].

Another significant finding revealed that ^{1}H-NMR spectra of malignant cells are remarkably similar to those obtained from activated immune cells, including mitogen-stimulated T-lymphocytes [49]. However, resting (unactivated) immune cells did not express the same relationship. Notably, both malignant cells and lymphocytes have the ability to migrate. Thus it has been suggested that elevated levels of membrane triglycerides are associated with an increase in cell motility [50]. The level of membrane lipid may correlate with the ability of malignant cancer cells to metastasize and the capacity of T-lymphocytes to migrate to the site of infection [38].

When studied by NMR spectroscopy, most cancer cells are characterized by increased narrow signals at 0.9 and 1.3 ppm corresponding, respectively, to methyl and methylene resonances that belong to isotropic lipid acyl chains. Acyl chains can form part of triglycerides or esterified cholesterol. Phospholipidic acyl chains may also be visible if they are not embedded in membrane lipid bilayers.

In model membranes, free cholesterol interacts with phospholipids and sphingolipids to influence membrane fluidity [51]. In vivo, cellular free cholesterol is located in the plasma membrane, which exhibits increasing structural order as demonstrated in erythrocytes [52] and CHO cells [53]. Moreover, cholesterol in model membranes is able to promote microdomains with less fluidity than the gel phase state and more fluidity than the surrounding membrane in the liquid crystalline state [54]. Therefore, there may be a link between increased cell motility and an increase in membrane fluidity that can be captured using NMR.

1.5. Summary

Humans consistently show a reduced response in the function of lymphocytes during and for several days after spaceflight; yet, we do not completely understand why. The normal T lymphocyte in the body kills host cells infected with bacteria or viruses and may rid the body of cancer cells. Stresses of space flight and other factors such as the increased growth rate of bacteria in microgravity and reduced immune cell function could increase danger from infections during long-term missions.

Studies have shown that the immune system is affected, and probably depressed during travel in space. In particular, lymphocyte number and function appear to be decreased in people and animals during space travel. However, the mechanism of how the immune system in depressed in space is poorly understood. The immune system is affected by many factors during space travel that may work together. These factors include physical and psychological stress, cosmic radiation, microgravity and changes in other physiological systems within the body.

We hypothesize that microgravity alters the mechanical force environment of lymphocytes. Evidence suggests that the cytoskeleton may function in "sensing" gravity at the single cell level. Spaceflight elicits a number of cell-level responses and some of these responses, including lymphocyte activation may involve the cytoskeleton. Changes in cytoskeleton protein expression may in turn affect signal transduction pathways, thereby causing altered cell function.

Previous research performed in our lab has shown that cells cultured in a low shear environment have increased cell motility and altered cell morphology. In particular, lymphocytes cultured in the rotating wall vessel (RWV) behave as if they have

been activated, which supports our hypothesis that cell function is changed in an altered mechanical force environment. Cell activation redistributes cell surface molecules and reorganizes the cytoskeleton. Motility changes may be modulated by prolonged stimulation of PKC occurring via PC cycles that generate second messengers such as DAG. We have hypothesized that fundamental changes in the cytoskeleton, caused by changes in external forces, could lead to secondary changes in cellular metabolism, which could in turn be reflected by altered membrane structure.

By utilizing NMR to investigate changes in lymphocyte function in an altered mechanical environment, our research seeks to advance understanding of how microgravity affects function of individual cells and how these cells interact with their environment.

2. LYMPHOCYTES CULTURED IN A ROTATING WALL VESSEL

2.1. Introduction

Experiments on space travelers suggest that the human immune system, and in particular lymphocyte function, is depressed in a microgravity environment. One possible explanation for these changes is that lymphocytes experience altered mechanical forces due to fluid redistribution in the body under microgravity conditions. However, the effects of mechanical forces on immune cells are poorly understood. As previously discussed, we believe that altered mechanical forces on lymphocytes in microgravity may affect cell function (cell adhesion, migration and activation). However, very little is known about how mechanical forces affect lymphocytes over an extended period of time. For this reason, we have studied the function of cells exposed to different environments of external mechanical forces. Over shorter periods of time, mechanical forces have been shown to affect leukocyte actin polymerization [55], homotypic aggregation [56, 57], and receptor affinity for ligand [58]. However, the systems used to study mechanical forces on cells over short periods of time (cone-plate viscometer and parallel plate flow chamber, for example) are not ideal for applying mechanical forces on cell for extended periods of time (days). For this reason, we have employed a Rotating Wall Vessel (RWV) to culture cells in a low shear mechanical environment.

2.2. Rotating Wall Vessel for Cell Culture

Since there are limited opportunities and technical difficulties associated with conducting biological research in space, efforts have been made to study the effects of

gravity on cells using terrestrial experiments. Unfortunately, a method has not yet been developed to eliminate the gravitational force on cells cultured on earth. Clinostats were the first cell culture system used to 'simulate' microgravity. A clinostat is loosely defined as any culture system that is rotated about a horizontal axis at a low rate of speed. The idea is that cells in the clinostat experience a gravitational force with constantly changing direction. Clearly, at any given moment, a gravitational force is exerted on each cell. By time averaging the gravitational force acting on cell revolving around a horizontal ais, however, the resultant or net gravitational force becomes zero.

Over the years, cell culture systems (generally termed rotating wall vessels (RWVs)) have been developed that consist of a tube filled with culture medium and suspended cells or tissues that rotates about a horizontal axis at a low angular speed [59]. These systems work on a similar premise as the clinostat, but with improved oxygen and nutrient delivery to the culture and well-characterized fluid dynamics [60, 61].

The question whether the clinostat (or RWV) is a reasonable ground-based model for microgravity has been debated in the gravitational biology field for many years. To answer this question, mechanisms of how cells sense microgravity must be considered. If cells sense gravity through a gravity receptor, then eliminating the net gravitational force by culture in a RWV may be a good model for microgravity. Thus, for the specialized plant cells that have been shown to sense microgravity through the movement of statoliths in the cell body, clinostat cell culture could be a good model for microgravity [62]. Although some investigators assert that RWV culture is a method for simulating microgravity, our hypothesis is that mammalian cells sense microgravity through changes in mechanical forces exerted on the cells and do not have a gravity receptor *per se*. If this

hypothesis is correct, then culture in the RWV is not necessarily a good model for microgravity, since the cells have no mechanism of sensing that the net gravitational force exerted on them has been eliminated.

Although the RWV does not simulate microgravity, it does offer a method of cell culture with characteristics that are significantly different than typical static cell culture. Two major types of the RWV have been developed: (1) the High Aspect Rotating Wall Vessel (HARV) and (2) the Slow-Turning Lateral Vessel (STLV). The HARV is a cylindrical rotating culture with a high aspect ratio and an oxygenation membrane at one end of the vessel. The STLV is the vessel used in our studies and is depicted in figure 2.1. In this vessel, the oxygenation membrane is at the center core of the vessel and air is pumped through the core. Both the HARV and STLV have been shown to support adequate oxygen transport capabilities for cell culture [63].

Some cells have shown an increased ability to attain three-dimensional structures in an RWV compared to conventional cell culture techniques [59]. This increase in three-dimensional aggregation of cells in the RWV has prompted researchers to study the growth of tissues in the RWV. Thus far, several tissues have been grown in RWVs including cartilage [63, 64], bone [65, 66], heart [67] and prostate [68] tissues. Also 3-D tumor tissues have been grown in the RWVs [69-71] and biological phenomena involving cell-virus contacts have been investigated [72, 73]. The goal of many of these studies is either to grow entire human organs in culture for transplantation or to study biological phenomena in three dimensions.

In our study, however, we have used the RWV cell culture system to investigate the effects of mechanical forces on single cells. The advantage of this system is that cells

can be cultured for an extended period of time in a controlled environment where they are exposed to low shear conditions. Thus, long-term effects of mechanical shear on cells or tissues can be studied. Since mammalian cells may sense microgravity through changes in mechanical forces exerted upon them, the function of cells after culture in the RWV is a potential ground-based method for elucidating the effects of microgravity on cell functions.

2.2.1. Fluid Dynamics in the Rotating Wall Vessel

Three dimensional fluid flow in rotating wall vessels and the effect of the fluid shear on cells cultured in RWVs has been well studied [76, 89 & 90]. Recently, Botchwey et. al. characterized the hydrodynamic conditions that occur during cell culture in a RWV using numerical simulation and imaging analysis [91]. Botchwey also observed that spherical particles with a density less than the surrounding fluid exhibited inward radial migration, while particles greater in density than the surrounding medium migrated outward in the radial direction. It has also been shown, that there is little influence of rotation frequency on instantaneous fluid speed. However, cell / microcarrier diameter does affect instantaneous speed [91]. That is, there is not a significant difference in the free fall particle speed and particle speed due to the solid body rotation of the fluid in the vessel, at least for the experimental conditions reported. Because of the solid body rotation, when the vessel is rotated the culture media rotates at the same angular velocity as the vessel wall with laminar fluid flow. In this environment, the damaging effects of turbulence and shear stress on cells are minimized.

Therefore, rotating wall vessels provide a low shear environment for cells [91-93]. According to the Stokes equation, the sedimentation velocity of a cell in a culture medium is inversely proportional to the viscosity and directly proportional to the difference in density between the cells and the fluid [91]. That is:

$$V = \frac{gd^2(\rho_c - \rho_m)}{18\mu} \qquad [2.1]$$

where g is acceleration due to gravity, d is the cell diameter, ρ_c is the cell density, ρ_m is the fluid medium density and μ is the viscosity of the fluid medium.

For our experimental environment, g = 9.81 m/s^2, d = 9.8 μm, ρ_c = 1003.394 kg/m^3, ρ_m = 993.36 kg/m^3 and μ = 7 g/m-s. Here we have assumed that the density and viscosity of the cell culture medium is that of water at 37 °C and that the density of a Jurkat cell is slightly higher than that of water. For these conditions and assuming that the rotational velocity of the RWV has a negligible impact on cell speed, the fluid velocity across the exterior surface of the cell is 7.495 x 10^{-8} m/s. Then, the shear stress on the exterior surface of the cell can be calculated [91] according to Stokes approximation:

$$\rho = -\frac{3\mu V}{2d} \qquad [2.2]$$

The minimum shear stress for our environment is approximately -0.08 g/ms^2, which is well below physiological shear stress caused by fluid flow in blood vessels. The physiological shear stress in blood vessels has been reported to be on the order of 1000-

2000 g/ms^2 [Westerhof, 2004]. It has been shown that cells cultured in a RWV have been shown to form cell aggregates, these aggregates can grow to be as large as 1mm in diameter [reference]. Shear stress estimates for aggregates are much more complex due to the flow of fluid over the exterior of the cells as well as interior fluid flow through the porous aggregate. Even for these larger aggregates (500 – 800 μm in diameter), the magnitude of cell speed is minimally affected by RWV rotation speed. Internal flow velocities for these larger aggregates have been reported to range from 0.2 mm/s to 13 mm/s, with maximum external shear stress values of 0.006 N/m^2 to 0.3 N/m^2. By comparison, maximum shear values on the interior of the cells aggregates varied from 0.007 N/m^2 to 0.03 N/m^2 [91].

2.2.2 Fluid Dynamics in Blood Vessels

In order to compare the low shear environment in the RWV with the physiological shear stress in blood cells it is instructive to discuss the fluid dynamics in blood vessels. Blood consists of plasma and particles, such as the red blood cells. The viscosity of blood thus depends on the viscosity of the plasma, in combination with the hematocrit (Ht). Higher hematocrit implies higher viscosity. The relation between hematocrit and viscosity is complex and many formulas exist. One of the simplest is the one by Einstein [94]:

$$\eta = \eta_{plasma} (1 + 2.5\, Ht) \qquad [2.3]$$

The viscosity of plasma is about 0.015 Poise (1.5 cP) and the viscosity of whole blood at a physiological hematocrit of 45 (%) is about 3.2 centipoise (cP).

The viscosity of blood depends on the velocity of the blood. More specifically, when velocity (shear rate) increases viscosity decreases. At higher velocity the disc-

shaped red blood cells (RBC's, erythrocytes) orient in the direction of the flow and viscosity is lower [94]. For extremely low shear rates, formation of RBC aggregates may occur, thereby increasing viscosity to very high values. It has even been suggested that a certain minimum shear stress is required before the blood will start to flow, the so-called yield stress. In large and medium size arteries shear rates are higher than 100 1/s, so viscosity is practically constant [94]. The physiological range of wall shear stress is 1000 to 2000 g/ms^2. The viscosity depends on the size of blood vessel. In small blood vessels, and at higher velocities, blood viscosity apparently decreases with decreasing vessel size. This effect begins to play a role in vessels smaller than 1 mm in diameter [94].

The anomalous character of blood viscosity results from the red blood cells, and the effects are mainly found in the microcirculation at low shear and small diameters [94]. The effects are of little importance for the hemodynamics of the larger arteries. Thus in hemodynamics it may be assumed that viscosity is independent of vessel size and shear rate.

2.3. Experimental Overview

Earlier studies in our laboratory found that RWV culture significantly affected cell migration, but did not affect cell adhesion [74]. This result was unexpected since differences in migratory characteristics are typically caused by changes in cell-substratum adhesiveness. Further tests suggested that the observed differences in migratory behavior between RWV and statically cultured cells were not caused by differences in integrin expression, membrane fluidity or cell cycle regulation [74]. To confirm these findings,

we decided to repeat the previous work by quantifying again the migratory behavior of Jurkat cells cultured in the RWV bioreactor and under static conditions.

2.4. Materials and Methods

2.4.1. Cells and Cell Culture

Jurkat cells (a T lymphoblastoid cell line) were used in adhesion and migration experiments. Jurkat cell suspensions were cultured in a complete media provided by American Type Cell Culture (ATCC, Manassas, VA): RPMI 1640 medium (ATCC), 10% fetal bovine serum (ATCC). RPMI formulation from ATCC contained 2 mM L-glutamine, 10 mM HEPES, 1mM sodium pyruvate, 4500 mg/L glucose and 1500 mg/L sodium bicarbonate. For general cell culture, cells were cultured on T-25 or T-75 tissue culture treated polystyrene flasks (Corning Inc., Corning, NY). Cells were maintained at 37 C in a humidified atmosphere containing 5% CO_2.

At 3-day intervals, the cells in culture were removed and placed in a new sterile tissue culture flask with fresh complete medium. Typically cells were seeded at a concentration of 5×10^5 cells/ml and did not exceed 2.2×10^6 cell/ml. Cell counting and viability were determined by trypan blue exclusion method using a Neubauer type hemocytometer.

2.4.2. Rotating Wall Vessel Cell Culture

Jurkat cells were cultured in suspension in a 55 ml Rotating Wall Vessel (RWV) (Synthecon, Houston, TX). This vessel, as depicted in Figure 2.1, consists of a cylindrical vessel oriented horizontally rotating around its z-axis. During cell culture, the

cylinder was completely filled with cells suspended in complete RPMI-1640 medium. As suggested by the manufacturer, the vessel was rotated at 10 RPM during cell culture. Ports allowing for fluid and cell suspension transfer to and from the vessel and removal

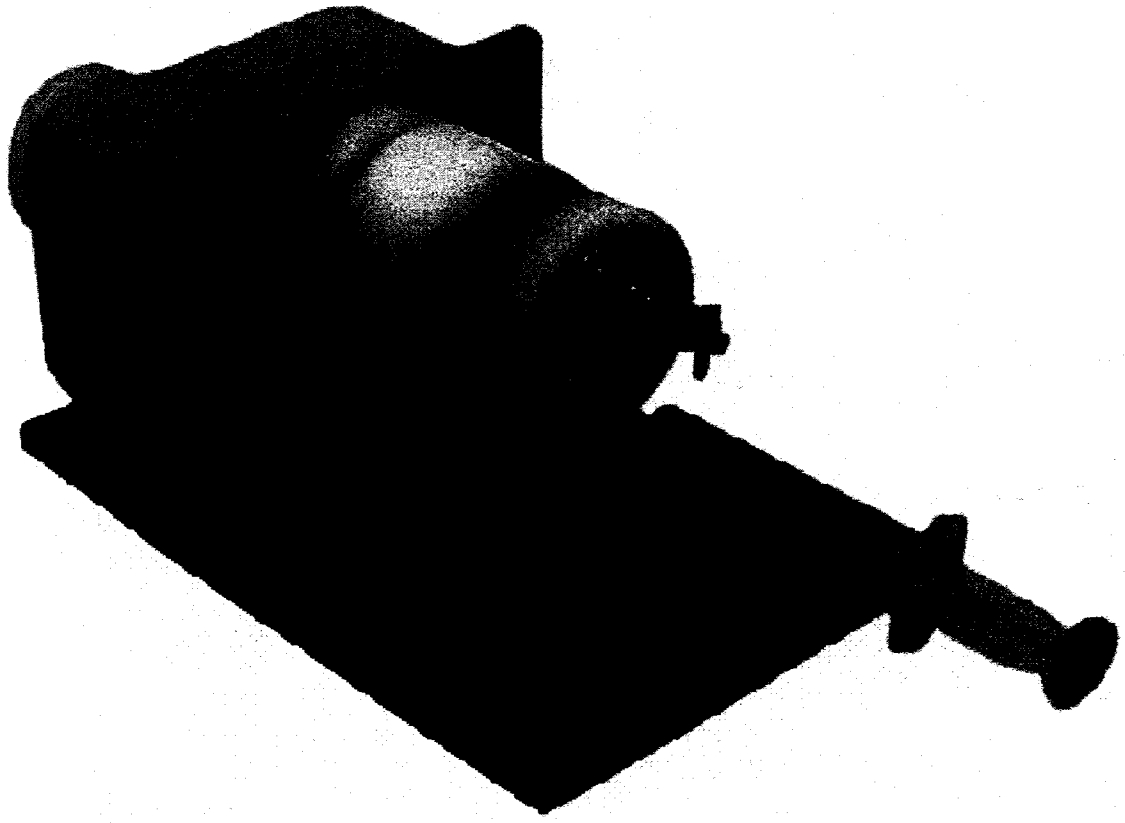

Figure 2-1: Rotating Wall Vessel
Jurkat cells were cultured in the RWV for up to 10 days. The RWV consists of a cylindrical vessel that rotates horizontally at a low rate (10 RPM for our experiments). Cells are oxygenated through a center oxygenation core which air is continuously pumped through. The vessel is completely filled with cell suspension in media. The apparatus is placed in an incubator for temperature, humidity and CO_2 control.

of any air bubbles from the RWV are located on the side of the vessel. A syringe filled with medium is kept on one of the ports during culture to allow for small volume changes that may occur in the vessel due to temperature changes or evaporation. The entire apparatus was placed in an incubator to allow for temperature, humidity and CO_2 control. Air was pumped through the center core of vessel allowing for gas transfer to and from the culture fluid.

To begin cell culture, approximately 1/3 of the vessel volume was filled with a Jurkat cell suspension at a concentration of approximately 1.9×10^6 cells/ml. Then, the vessel was completely filled with complete RPMI-1640 medium to give a concentration of approximately 5.5×10^5 cells/ml. Air bubbles were then removed from the vessel by injecting a small amount of complete media into one of the ports while allowing the air to escape through another port. The culture vessel was screwed onto the motor and the whole apparatus was placed in an incubator. The vessel was then rotated continuously at 10 RPM.

Once cell culture in the RWV began, cell culture was interrupted at 3-day intervals to adjust the cell concentration and test cell viability. The RWV was removed from the motor and an appropriate amount of Jurkat cell suspension was removed from the vessel. Only a small portion of this suspension was used for experiments, and the rest was discarded. Cell concentration was adjusted to 5.5×10^5 cells/ml with fresh complete RPMI-1640 medium and bubbles were removed from the vessel as previously described. The RWV was then connected to the motor in the incubator once again for 3 more days of continuous culture at 10 RPM. For the studies presented here, the cells were cultured for up to 12 days in this manner.

Jurkat cells were cultured in the RWV concurrently with statically cultured cells; i.e, when RWV cultured cells were sampled, cells cultured on tissue culture plates were also sampled. For the experiments presented here, Jurkat cells were sampled from the RWV at 3-day intervals and compared to cells cultured statically on tissue culture plates.

2.4.3. Video Microscopy Setup

The video microscopy setup used to study cell function was previously developed [78-80] and was utilized for adhesion and migration experiments in this study with some minor modifications. The setup consists of a microincubator mounted on a motorized stage (LEP Limited, Hawthorne, NY) of an inverted light microscope (JENA, Sedival, Seiler Instruments Co., Dallas, TX). Briefly, the microincubator was machined from a solid block of aluminum and had a lexan cover to allow for sample removal and loading. A glass microscope slide fixed at the bottom of the incubator allowed for passage of incident light. The incubator was kept at 37°C using two external heaters and a proportional temperature controller (Cole-Parmer Instrument Co., Chicago, IL, Digisense). To maintain optimal cell culture conditions, air containing 5% CO_2 was flushed through the incubator at 10-minute intervals. A black and white digital camera (XC-77, Sony, Tokyo, Japan) was mounted on the inverted light microscope to allow for the capture of gray-scale images during the experiment.

A computer (PowerMac 8500, Apple, Cuppertino, CA) was used to operate a Labview 5.0 program previously developed [74, 79]. This setup was used to control movement of the stage, flow of air through the incubator and the triggering of image capture by a second computer (G5 MacIntosh, Apple) equipped with a frame grabber

card (AG-5, Scion Corp., Frederick, MD). At the appropriate time, the control computer directed the stage to the desired location, focused the image and signaled image capture by the G5 MacIntosh. The system was calibrated such that adjacent images in both the vertical and horizontal directions could be captured.

An image acquisition program (Scion Image 1.59, Scion, variant of NIH Image) was used on the G5 MacIntosh to capture and splice images together. Coordinated with the control computer, the acquisition computer used a macro developed to capture digital images upon a triggering signal from the control computer after the stage was moved to the proper location. This macro was also used to splice images together and save the images to the hard drive for future analysis.

2.4.4. Preparation of Fibronectin-Coated Surfaces for Experiments

Stock fibronectin solutions were prepared by adding sterile distilled water to lyophilized human plasma fibronectin (Life Technologies) to achieve a solution of 1 mg fibronectin/ml. This stock solution was stored at 4°C for up to two weeks or frozen at –20°C for extended periods of time. Fibronectin solutions for surface preparations were made by diluting stock fibronectin solutions with sterile PBS to obtain a working concentration 4.3 μg/ml.

Polystyrene surfaces for migration experiments were prepared using 96-well tissue culture treated plates (Corning). From each 96-well plate, 2 2x8 strips of wells were removed from the edges of the plate by cutting aseptically with a hot knife. Six wells of the 16 in the strip were used for migration experiments (see Figure 2.2).

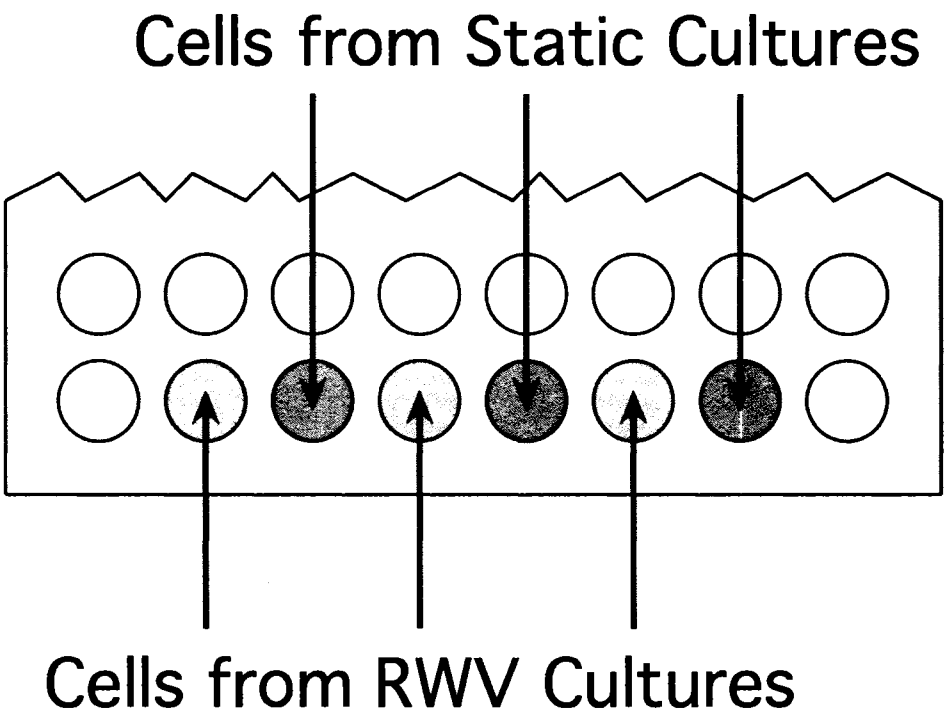

Figure 2-2: Cell Migration Set-up
A strip was cut from 96-well plates as depicted here. The 6 wells used for migration experiments were treated with fibronectin and the strip was placed in the microincubator. Cells from RWV and static cultures collected on the same day were assayed simultaneously and in triplicate to minimize variability in the measurement of migration parameters [74].

To prepare fibronectin-coated surfaces, 100 µl fibronectin solution aliquots of appropriate concentration were added to each of the six wells used for migration experiments and incubated at 37°C for 2 hours. The plates were then washed twice with sterile PBS and incubated with 2% bovine serum albumin solution in PBS for 1 hour at 37°C to block any remaining binding sites. Finally, the surfaces were washed twice with PBS and used for migration experiments.

2.4.5. Cell Migration Experiment

Jurkat cells were taken from culture and diluted in complete RPMI-1640 medium supplemented with 3% carboxy-methyl-cellulose solution to a concentration of 20 cells/µl. Cell concentrations were attained by measuring cell concentrations using a hemocytometer and performing the appropriate dilutions. Using this approach, the cells are never 'washed' by centrifugation and removal of used medium. However, using our culturing method, the concentration of cells removed from suspension was on the order of 4000 cells/ml. Thus, only a very small percentage of the used medium remained in the cell suspension used for migration experiments.

The diluted cell suspension (20 cells/µl) was then added in 100 µl aliquots to each of the six wells in the prepared polystyrene strip (as described in the previous section). The plates were then incubated at 37°C for 30 minutes to allow the cells to settle and attach to the fibronectin-coated surface. The strip containing the cells was then placed in the microincubator on the stage of an inverted light microscope of the video microscopy setup described above. A small amount of water (~15 ml) was placed in the bottom of

the microincubator to increase the humidity in the incubator and to improve the temperature control.

An image processing program (Scion Image 1.59) was used to capture and analyze digital images. At 10-minute intervals, 12 adjacent digital images (forming a 3 x 4 mosaic) from each of the six wells were acquired and spliced together to form a larger image (1920 x 1920 8-bit pixels) covering an area equal to 1.33 mm^2. Each pixel size was determined to be 0.6 μm/pixel in both the x and y directions using a microruler. This process continued for 7 hours. Thus, at the conclusion of the experiment, 45 digital image mosaics of each well were recorded to reconstruct cell trajectories and examine cell migratory characteristics.

2.5. Results and Discussion

The following results (Figures 2.3 - 2.6) support the findings from previous studies performed in our laboratory [74]. Figure 2.3 depicts the average cell speed V of Jurkat cells after 0-10 days of culture in the RWV. Cell speed V is determined by averaging the measured individual cell speeds (V_k) of all cells tracked (100 cells in our experiments)

$$V_k = \frac{\sum_{j=1}^{N} d_j}{N \cdot \Delta t} \qquad [2.4]$$

where N is the displacements of the cells and Δt is the time interval between image acquisitions [79].

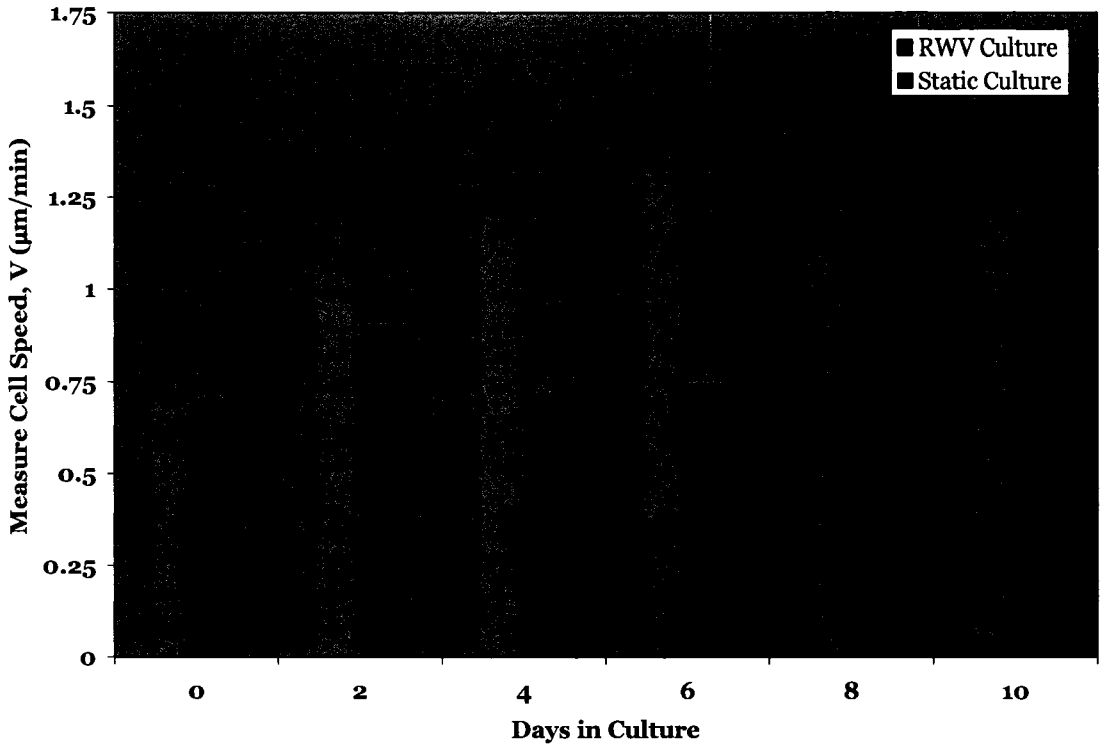

Figure 2-3: Effect of RWV Culture on Cell Speed, V
Jurkat cells were cultured in the RWV or statically for 0-10 days and then plated on fibronectin (4.3 μg/ml) or collagen (100 μg/ml)-coated surfaces at 2-day intervals, as indicated. Measured cell speed was then determined using the methods outlined in section 2.3.3. Migration experiments on collagen-coated surfaces were only performed after 6 days of culture. The measured cell speed of RWV cultured cells was significantly higher after 4-10 days in culture. The error bars represent the standard deviation of the 3 experimental trials.

After 2 days of culture in the RWV, a small increase in the cell speed V was observed on fibronectin-coated surfaces. After 4-10 days of culture in the RWV, however, Jurkat cells exhibited a significantly higher cell speed (approximately 2-fold increase) than cells cultured statically. Furthermore, the cell speed exhibited by Jurkat cells cultured in the RWV reached a plateau after 4 days in culture (see Figure 2.3). On the other hand, cell speeds of statically cultured cells did not vary with time in culture.

Similar to the cell speed V, cells cultured in the RWV exhibited a higher RMS cell migration speed S than cells cultured statically. RMS migration speed is the instantaneous cell speed, obtained along with persistence P (the characteristic time between directional changes) by plotting the mean squared displacement $\langle D^2 \rangle$ of a population of cells over time and fitting the data to the following equation [79]:

$$\langle D^2 \rangle = 2S^2 P\left\{t - P\left[1 - \exp\left(-\frac{t}{P}\right)\right]\right\} \qquad [2.5]$$

Equation (2.9) describes persistent random walk in two-dimensions and assumes that RMS cell speed S, and the persistence of cell movement, P, do not vary with time. These two parameters can be combined to define a random motility coefficient μ which is the effective diffusion coefficient over large time periods [79]:

$$\mu = \frac{1}{2} S^2 P \qquad [2.6]$$

For our experiments, mean squared displacement curves were determined as follows:

$$\langle D^2 \rangle = \frac{1}{N} \sum_{1}^{N} d_{i,t}^2 \qquad [2.7]$$

where N is the number of cells in the population and d_i is the displacement of a single cell at time t [74].

The RMS cell migration speed plotted versus time in culture is depicted in Figure 2.4. Again, after 4 days of culture in the RWV, the RMS cell speed reached an apparent maximum at approximately 2 times the speed of cells that were previously cultured statically. Although the effect on cell speed was greatest after 4-10 days in cell culture, the RMS cell speed of cells cultured in the RWV for two days was also higher than statically cultured cells.

Figure 2.5 shows the effect of RWV cell culture on the persistence time of Jurkat cells migrating on fibronectin-coated polystyrene. The persistence times of statically and RWV cultured cells exhibited no statistically significant differences after 2 days of culture. After 4-10 days in culture, however, RWV cells showed a significantly lower persistence than cells cultured statically. Again, this effect appeared to plateau after 4 days in culture. Thus, cells cultured in the RWV showed a higher speed, but they change direction of migration much more often than statically cultured cells.

Figure 2.6 depicts the effect of culture method on the random motility coefficient. Although the persistence time is decreased in RWV cultured cells, the random motility coefficient showed a significant increase 4-10 days after cell culture. The random motility coefficient also showed a slight increase after two days of culture. Thus, the effect of increased cell speed overcame the decreased persistence time of RWV cultured cells resulting in increased random motility coefficients.

To determine if the cells cultured in the RWV spread differently than statically cultured cells, the size and morphology of cells on fibronectin-coated surfaces were

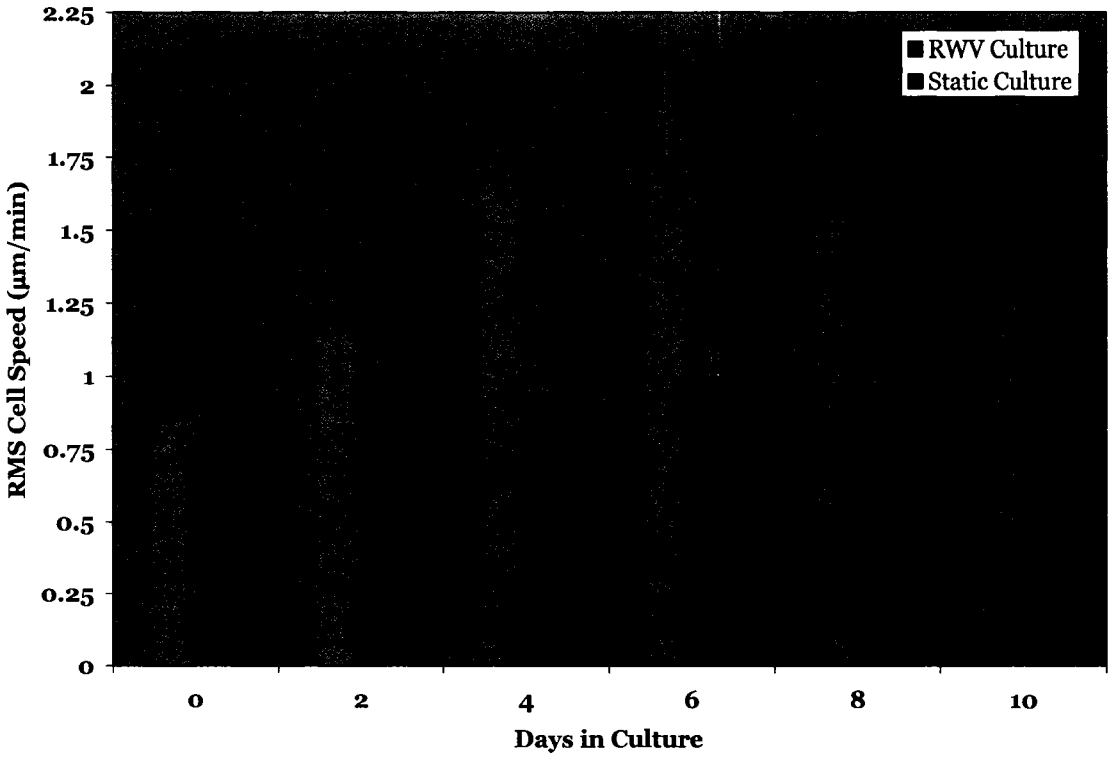

Figure 2-4: Effect of RWV Culture on RMS Cell Speed
Jurkat cells were cultured in the RWV or statically for 0-10 days and the cells were sampled and assayed at 2-day intervals. The cells were plated on fibronectin-coated surfaces prepared with a fibronectin solution concentration of 4.3 μg/ml as described in section 2.3.3. Jurkat RMS cell migration speeds were determined on these surfaces after RWV culture using the persistent random walk model. RMS cell speeds of RWV cultured cells were significantly higher than statically cultured cells after 4-10 days of culture. The error bars represent the standard deviation of the 3 experimental trials.

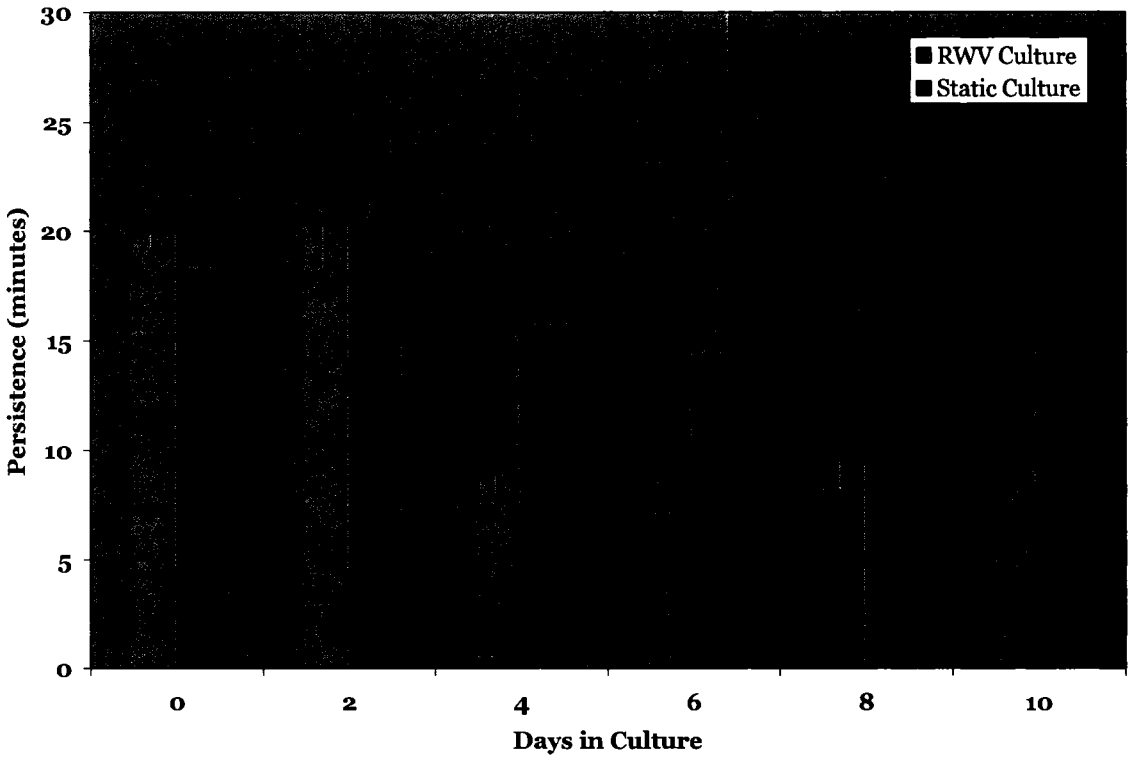

Figure 2-5: Effect of RWV Culture on Persistence Time

Jurkat cells were cultured in the RWV or statically for 0-10 days and the cells were sampled and assayed at 2-day intervals. The cells were plated on fibronectin-coated surfaces prepared with a fibronectin solution concentration of 4.3 μg/ml as described in section 2.3.3. Persistence times were determined for Jurkat cells on these fibronectin-coated surfaces after RWV culture using the persistent random walk model. Persistence times were significantly lower for RWV cultured cells 4, 8 and 10 days after the onset of culture. The error bars represent the standard deviation of the 3 experimental trials.

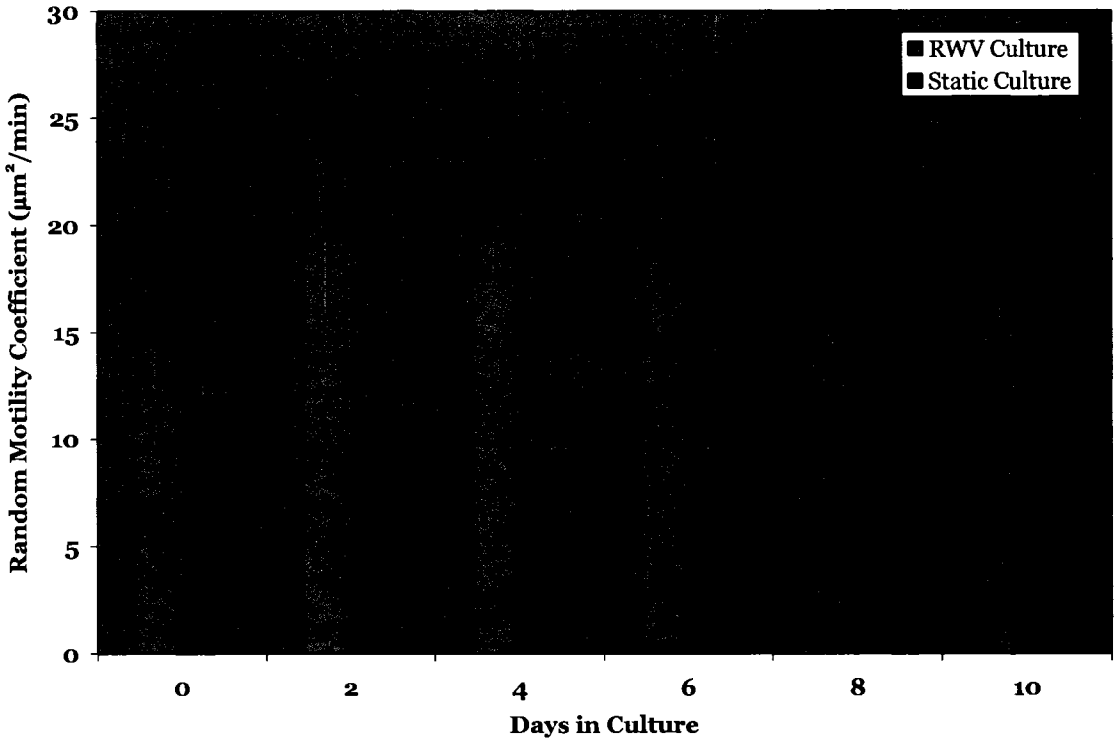

Figure 2-6: Effect of culture conditions on Random Motility Coefficient
Jurkat cells were cultured in the RWV or statically for 0-10 days and the cells were sampled and assayed at 2-day intervals. The cells were plated on fibronectin-coated surfaces prepared with a fibronectin solution concentration of 4.3 μg/ml as described in section 2.3.3. Random motility coefficients were then determined for Jurkat cells on these fibronectin-coated surfaces after RWV culture using the persistent random walk model. The random motility coefficient of RWV cultured cells were significantly higher than statically cultured cells 4-8 days after the onset of culture. The error bars represent the standard deviation of the 3 experimental trials.

examined previously in our laboratory [74]. Differences in cell spreading may indicate changes in the cytoskeleton of the cell and/or differences in focal contact formation and cell adhesion characteristics. After 6 days of RWV culture, Jurkat cells exhibited a significantly lower projected cell area than statically cultured cells, results not shown here. Furthermore, RWV cultured cells exhibited a less round morphology (corresponding to a higher morphology index) than cells cultured statically.

As previously discussed in section 1.3, lymphocyte function is impaired in microgravity, possibly due to altered mechanical forces on single cells. Our results show that mechanical forces may significantly affect cell migration, a crucial step in the lymphocyte immune response. A well-known mechanism of how cells can modulate cell migration characteristics is by modulation of cell-substrate adhesion characteristics [82-84]. However, using a parallel plate flow system, we determined previously that Jurkat cell adhesion to fibronectin was not significantly affected by previous culture in the RWV for 6-10 days. These experiments suggest that the altered migratory behavior of Jurkat cells cultured in the RWV is not due to changes in cell-substrate adhesion strength, but rather to some other mechanism.

In previous studies performed in our lab, several possible hypotheses were suggested and tested in an effort to explain the altered behavior of cells cultured in RWV bioreactors. These hypotheses included inhibition of cell-substratum contacts, differing immediate nutritional environments, cell cycle regulation, altered expression of cell surface receptors, and altered signaling pathways [74].

These studies revealed, however, that none of the proposed mechanisms could account for the altered migratory behavior of cells cultured for more than 4 days in an

RWV bioreactor. Thus, further studies are needed to elucidate the mechanism through which mechanical forces affect the biochemical pathways in Jurkat cells after RWV culture. In the next chapter we will discuss the use of NMR spectroscopy helping an effort shed some light on the altered migratory behavior observed after RWV culture.

3. ^{1}H-NMR INVESTIGATION OF LYMPHOCYTES CULTURED IN A ROTATING WALL VESSEL

3.1. Introduction

Previous studies performed in our laboratory indicated that culturing lymphocytes under low shear conditions in rotating wall vessels (RWV) leads to an increase in cell motility and altered cell morphology [74]. These studies also showed that the observed differences in migratory behavior between RWV and statically cultured cells were not caused by differences in integrin expression, membrane fluidity or cell cycle regulation [ibid].

In this section, we will investigate the validity of another possible explanation. As has been observed with malignant cells, motility changes may be modulated by prolonged stimulation of protein kinase C (PKC) occurring via phosphatidylcholine (PC) cycles that generate second messengers such as diacylglycerol (DAG) [87]. It is thus possible that changes in the cytoskeleton caused by changes in external forces, could lead to secondary changes in cellular metabolism, which could in turn be reflected by altered membrane structure. Several recent studies suggest that the synthesis of NMR-visible ML in activated lymphocytes is linked to the PC cycle [44].

Using ^{1}H-NMR spectroscopy to measure the levels of mobile lipid, we observed previously in our laboratory that lymphocytes cultured in the RWV had remarkably similar spectra to those obtained from malignant cells [44]. This observation raised the possibility that a common "activation" pathway exists for malignant cells and lymphocytes activated by either chemical stimuli or mechanical forces. Notably, both

malignant cells and lymphocytes have the ability to migrate and thus elevated levels of MNL may be associated with an increase in cell motility. The level of membrane lipid may correlate with the ability of malignant cancer cells to metastasize and the capacity of T-lymphocytes to migrate to the site of infection.

Furthermore, there is emerging evidence that the structural changes in the cytoskeleton (membrane fluidity) may play an important role in modulating the activity of PKC [43]. In fact, since the structure and function of membrane proteins depends on the lipid environment any perturbation of the cytoskeleton inevitably affects PKC activity [43, 44].

3.2. Experimental Overview

In this study, ^{1}H-NMR was used to explore structural changes indicated by a high resolution signal arising from neutral lipids (or lipid visibility) in the cytoskeleton of Jurkat cells that were cultured in the RWV bioreactor.

3.3. Material and Methods

3.3.1. Cell Culture

Jurkat cells were cultured in the RWV concurrently with statically (T-flask) cultured cells as described in the previous chapter. For the experiments presented here, Jurkat cells were sampled from the RWV and compared to cells cultured statically on tissue culture plates after 12 days. Typically cells were seeded at a concentration of 5 x 10^5 cells/ml and did not exceed 2.2 x 10^6 cell/ml. Cell counting and viability were determined by trypan blue exclusion method using a Neubauer-type hemocytometer.

3.3.2. ^{1}H-NMR Sample Preparation

A sample (~2ml) of cells was taken from each culture vessel and counted to determine the appropriate volume of cell suspension needed to obtain a total of 5 x 10^7 cells. Each cell suspension was placed in a 50 ml modified polystyrene centrifuge tube (Corning, Corning, NY) and centrifuged (Sorval refrigerated centrifuge, Wilmington, DE) at a speed of 600 rpm at 4 °C. To prevent any further metabolic changes cell samples were kept on ice. The supernatant was carefully removed with a glass pipette (lengthened with a Bunsen burner) and the cell pellets were re-suspended in 1-2 ml of PBS in 99.9% D_2O (Sigma). Centrifugation was repeated in order to remove as much water as possible. The final cell pellets were re-suspended in 500 µl of PBS in D_2O before being transferred to a 5 mm Wilmad NMR tube.

3.3.3. ^{1}H-NMR Measurements

Two sets of NMR experiments were performed in our laboratory. The first set of experiments used an AMX 500 MHz spectrometer (Bruker) with a H probe to collect ^{1}H 1D spectra. The second set of ^{1}H 1D spectra were collected using Inova 500 and 600 MHz spectrometers (Varian, Inc.) equipped with inverse Penta and inverse HCN probes respectively. Each set of experiments used sample volumes of 600 µL in 99.9% D_2O. A small amount of 2,2-dimethyl-2-silapentane-5-sulfonic acid (DSS, 0.25 mM) was added as a proton referencing standard for experiments performed on the Inova 500 and 600 spectrometers. On experiments using DSS, the magnet was shimmed to give a 1-2 Hz linewidth on the DSS methyl proton peak. In the same set of experiments, EDTA was added to 50 µM EDTA in one sample to test for the presence of paramagnetic metal ions. Since there was no change in linewidth of the DSS standard, EDTA was not included in

subsequent samples. In all experiments Wilmad 528-PP or 535-PP NMR tubes (5 mm OD) were used. Typical data collection parameters were at 12-13 ppm sweep width, a 5 second interpulse delay, a presaturation pulse of 0.5-0.75 sec, a 6.5 (Inova 500) or 9 (Inova 600) microsecond 90 degree pulse, and a 4 second acquisition time. Low signal-to-noise spectra were collected with 16 scans; longer acquisitions collected 256 scans. To check the effect of sample stability (cell settling) on the spectra during acquisition, 128 scans were collected at 600 MHz as 8 spectra of 16 scans each, and the first and last 16 scan spectra were compared before adding all 8 spectra together to increase signal to noise. A similar procedure was performed in the first set of experiments on the AMX 500 MHz spectrometer.

3.3.4. ^{1}H-NMR Data Processing

For all experiments, signal processing and quantitative data analysis of the one-dimensional (1D) ^{1}H-NMR spectra was performed using the Felix software package. The model used to approximate the measured free induction decay (FID) was the sum of the complex exponentially damped sinusoids. Pre-processing of the FIDs consisted of removal of residual water signal; 0.5 Hz line broadening was applied.

3.4. Results and Discussion

3.4.1. ^{1}H-NMR Data Analysis

Figure 3.1 is an example from the initial NMR analysis performed in our laboratory using the AMX 500 MHz spectrometer (section 3.3.3). The top portion of the figure represents a Jurkat cell sample cultured for 12 days in the RWV and the lower

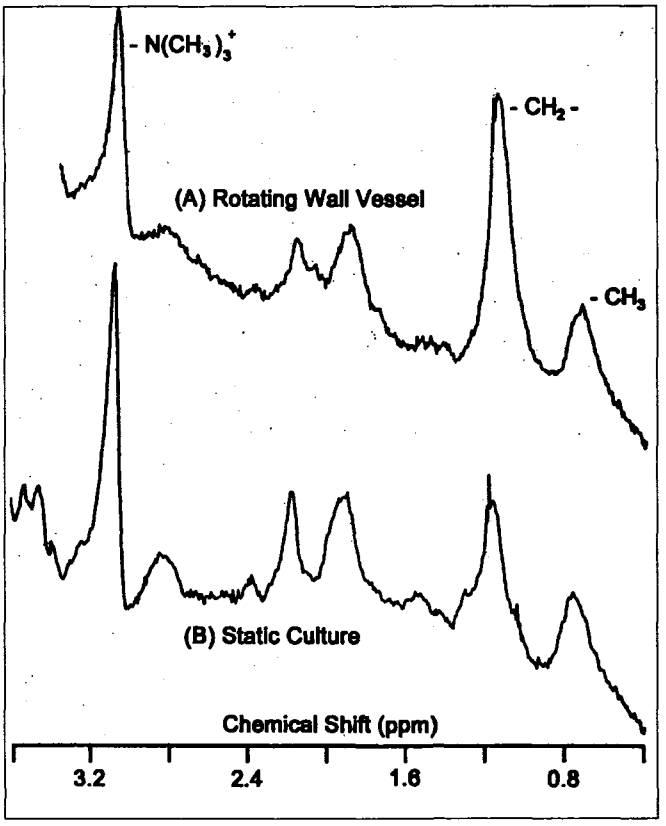

Figure 3-1: Comparison of spectra from Jurkat cells cultured in a RWV and statically (control).

portion of the figure represents a static sample (control). The peaks of interest are labeled, from left to right, choline [$N(CH_3)_3$], 3.2 ppm; methylene [$(CH_2)_n$], 1.3 ppm and methyl [CH_3], 0.9 ppm.

From this figure, it can be observed that there is an increase in the signal intensity of methylene and a decrease in the signal intensity of choline, relative to the control, for cells cultured in the RWV after 12 days. This signal intensity is represented graphically in Figure 3.2. Peak (signal) intensities were calculated by measuring (utilizing Felix NMR processing software) the area of each peak. It can be seen in Figure 3.2 that the methyl peak intensity is constant for both Jurkat cells cultured in the RWV and for static samples. For cells cultured under low shear conditions, the methylene peak intensity increased and the choline peak intensity decreased compared to cells cultured statically.

An alternative way to express the change in lipid signal intensity is by using a peak area ratio. Recall that the methyl peak intensity is constant for both Jurkat cells cultured in the RWV and for static samples. This methyl peak stability is in agreement with experiments performs by others [87]. The CH_3 resonance at 0.9 ppm is well defined due to relatively mobile protons, and is unlikely to be affected by dynamic changes in the plasma membrane. Therefore, we will use the peak area ratio to express the change in methylene and choline signal intensity relative to the methyl signal intensity, which is constant for both static and low-shear conditions.

For RWV cultured cells, peak intensity ratios for choline / methyl and methylene / methyl were 2.35±0.39 and 2.81±0.51, respectively (Figure 3.3). For cells cultured statically, the ratios were 3.88±0.61 and 1.88±0.20, respectively. The differences between the RWV cultured cells and statically cultured cells were statistically significant

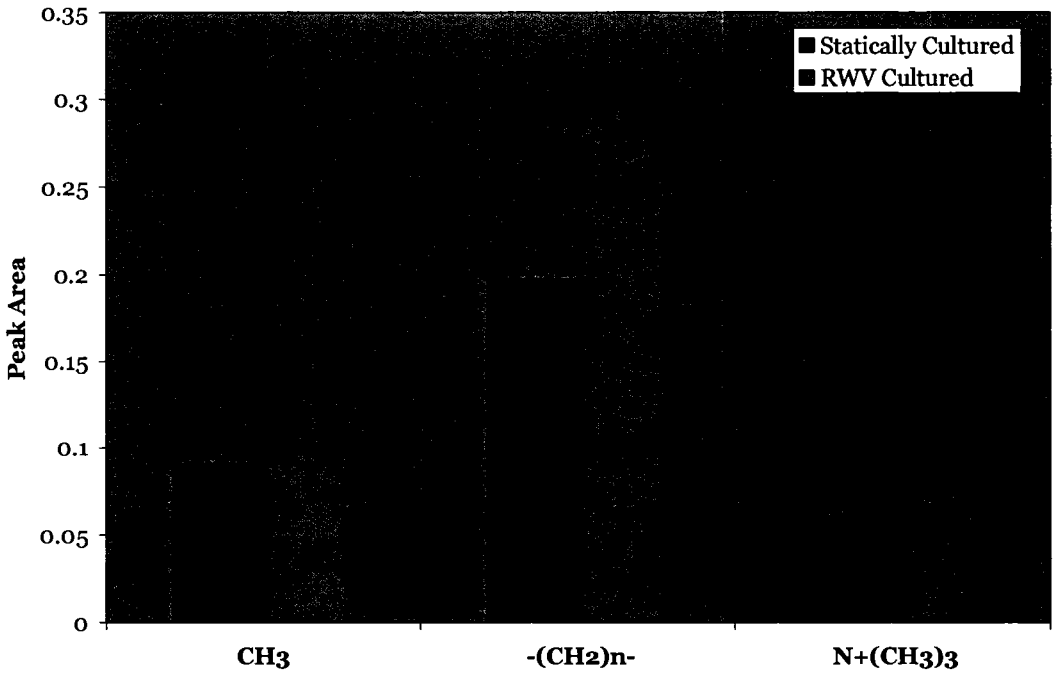

Figure 3-2: Peak area for cells cultured for 12 days under (a) static and (b) low-shear conditions in a RWV reactor.
$N^{+}(CH_3)_3/CH_3$, n = 3, $p<0.001$; $(-CH_2-)n/CH_3$, n = 3, $0.001<p>0.01$]. The error bars represent the standard deviation of the 3 experimental trials.

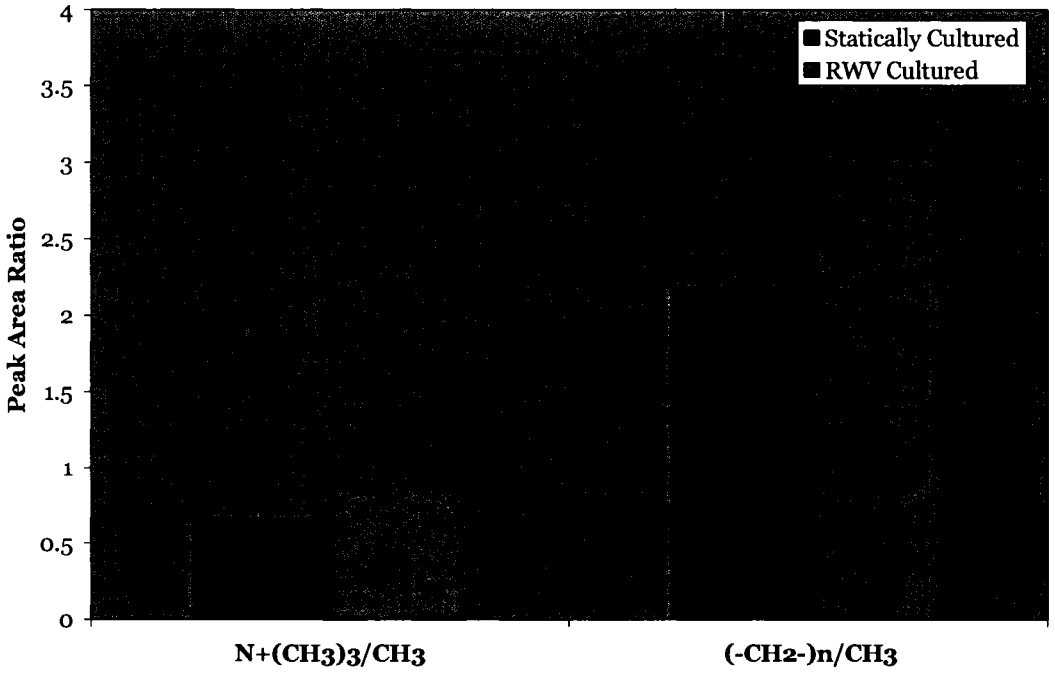

Figure 3-3: Peak area ratios for cells cultured for 12 days under (a) static and (b) low-shear conditions in a RWV.
$[N^{+}(CH_3)_3/CH_3$, n = 3, $p<0.001$; $(-CH_2-)n/CH_3$, n = 3, $0.001<p>0.01]$. The error bars represent the standard deviation of the 3 experimental trials.

for both the choline / methyl ratio ($p<0.001$) and the methylene / methyl ratio ($0.001<p<0.01$), as determined by a double tailed Student's t-test. From each culture method, 3 samples were extracted. Three ^1H NMR measurements were taken for each sample and the experiments were repeated 3 times.

The resonances where changes were observed are all related to phospholipid metabolism [85]. The shift from choline to methylene has been linked to the formation of highly mobile neutral lipids (MNL's), located in separate area in the cell membrane or in lipid droplets in the cytoplasm. The exact subcellular location of MNL's is still a matter of debate [86]. In general, an increase in MNL's is observed when cells are under some form of stress. This phenomenon has been observed during apoptosis [87] and lymphocyte activation [44], as well as in embryonic cells [88]. CH_3 resonances have been shown to not be greatly affected by dynamic changes of the plasma membrane [87]. Similarly, the $N^+(CH_3)_3$ protons from the phospholipid head groups are not affected significantly [ibid]. It is plausible that the decrease in choline / CH_3 signal intensity ratio may be due to the loss of choline not related to the lipid bilayer [ibid]. It is also interesting to note that it has been reported that there is a correlation between apoptosis and an increase in methylene / CH_3 signal peak intensity [ibid]. It is possible that the loss of cytoskeletal architecture is partly responsible for changes in lipid expression. The loss of cytoskeletal structure may allow for increased mobility of the plasma membrane lipids.

The changes in MNL levels in cells grown under low shear conditions suggests that the cells undergo a change in cell membrane composition and structure. In Chapter 2 we confirmed that cells cultured under low shear conditions exhibited increased cell speed [74]. How the membrane change could be related to cell motility is a very

interesting but still unanswered question. One might speculate that fundamental changes in the cytoskeleton, caused by changes in external forces, could lead to secondary changes in cellular metabolism, which could in turn be reflected by altered membrane structure.

Furthermore, researchers [85] have shown that cells with decreased cholesterol content exhibit similar spectra to those obtained in the current study from cells cultured in a low shear environment. In model membranes, free cholesterol interacts with phospholipids and sphingolipids to influence membrane fluidity [85]. *In vivo*, cellular-free cholesterol is located in the plasma membrane, which exhibits increasing structural order as demonstrated in erythrocytes, LM and CHO cells [85]. Moreover, cholesterol in model membranes is able to promote microdomains towards an intermediate state called the liquid-ordered phase, with less fluidity than the gel phase state and more fluidity than the surrounding membrane in the liquid crystalline state [85]. In our experiments we observe there is a marked shift from choline to methylene signal intensity. This decrease in choline peak intensity could correlate with a decrease in cholesterol content, thus resulting in increased membrane fluidity. This correlation would be in agreement with our current results of increased motility due to RWV culture. These results demonstrate that a ^{1}H-NMR spectrum can provide useful qualitative information about changes in lymphocyte cell metabolism and membrane fluidity.

In the first set of experiments (performed on the AMX 500 MHz spectrometer) there were significant peak overlaps in our spectra. This peak overlapping makes it difficult to accurately integrate the areas of lipid resonances. In order to more accurately determine MNL concentrations, further experiments were performed utilizing more

advanced NMR instruments (Inova 500 and 500 MHz spectrometers, see section 3.3.3). In this series of experiments, a reference, 2,2-dimethyl-2-silapentane-5-sulfonic acid (DSS), was added in a known molar concentration to the Jurkat cell suspension before acquisition. The DSS reference added in a known molar concentration allowed us to quantify changes in lipid concentrations. In addition to quantifying the amount of MNL, the time course of the change undergone by the Jurkat cells cultured in a low shear environment was captured. Jurkat cell samples were taken from the RWV and static flask (control) every 3 days, beginning on the 3rd day and continuing for 12 days (the length of previous NMR experiments performed in our laboratory.)

Figure 3.4a-h shows the result of this series of experiments. The peaks of interest, from left to right, indicated by arrows, are choline [$N+(CH_3)_3$], 3.2 ppm; methylene [$(CH_2)_n$], 1.3 ppm and methyl [CH_3], 0.9 ppm, with additional peaks representing the standard (DSS) at 2.9, 1.7, 0.7 and 0 ppm, respectively. Spectra a-d (left) represent cells cultured statically (control) and e-h (right) represent cells cultured under low shear conditions (RWV). Each spectrum represents a 3 day time period, i.e., spectra a & e were captured following three days of cell culture, spectra b & f were captured after 6 days, and so forth, continuing through 12 days (d & h).

The spectra produced in the time course set of experiments appear to be significantly different than those obtained previously (Figure 3.1). Since the methyl peak intensity is the same for both static and RWV cultured cells we have used the peak height ratio to compare the time course (current) experiments with the first set of experiments. We have calculated the peak area ratios for spectra obtained following 6, 9 and 12 days of culture and these results are represented graphically in Figures 3.5-3.7.

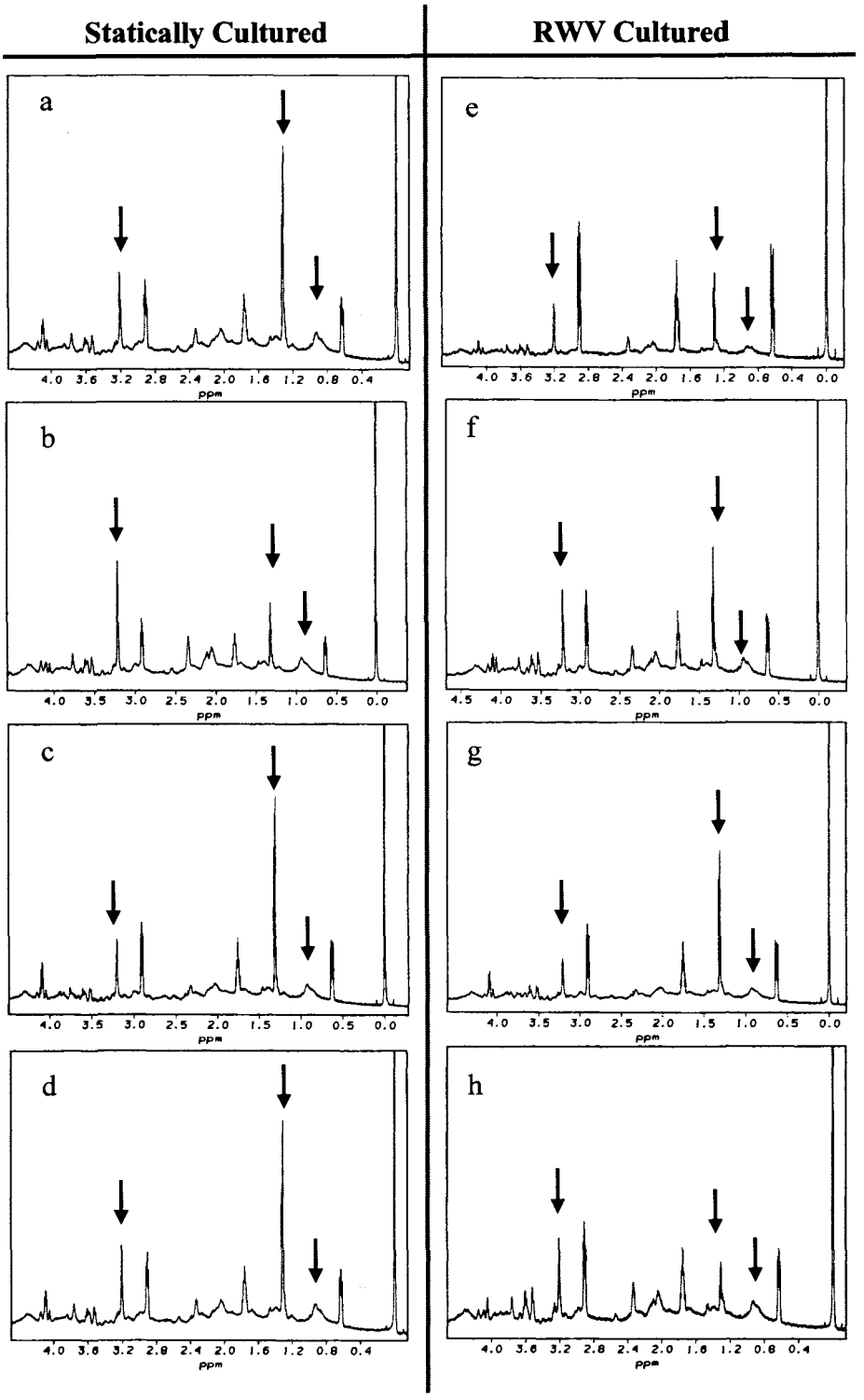

Figure 3-4a-h: Time course study of Jurkat cells cultured under static and low shear conditions. Arrows indicate peaks of interest: $[N+(CH_3)_3]$, 3.2 ppm; methylene $[(CH_2)_n]$, 1.3 ppm and methyl $[CH_3]$, 0.9 ppm.

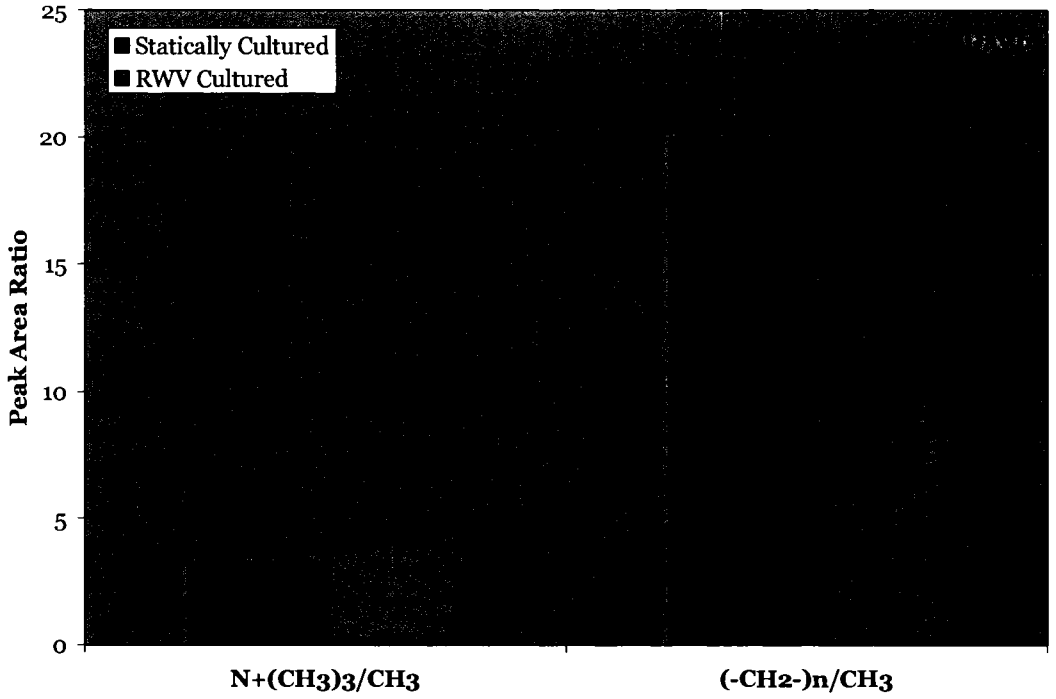

Figure 3-5: Peak area ratios for cells cultured for 6 days under static and low-shear conditions. [$N^{+}(CH_3)_3/CH_3$, n = 3, $p<0.001$; $(-CH_2-)n/CH_3$, n = 3, $0.001<p>0.01$]. The error bars represent the standard deviation of the 3 experimental trials.

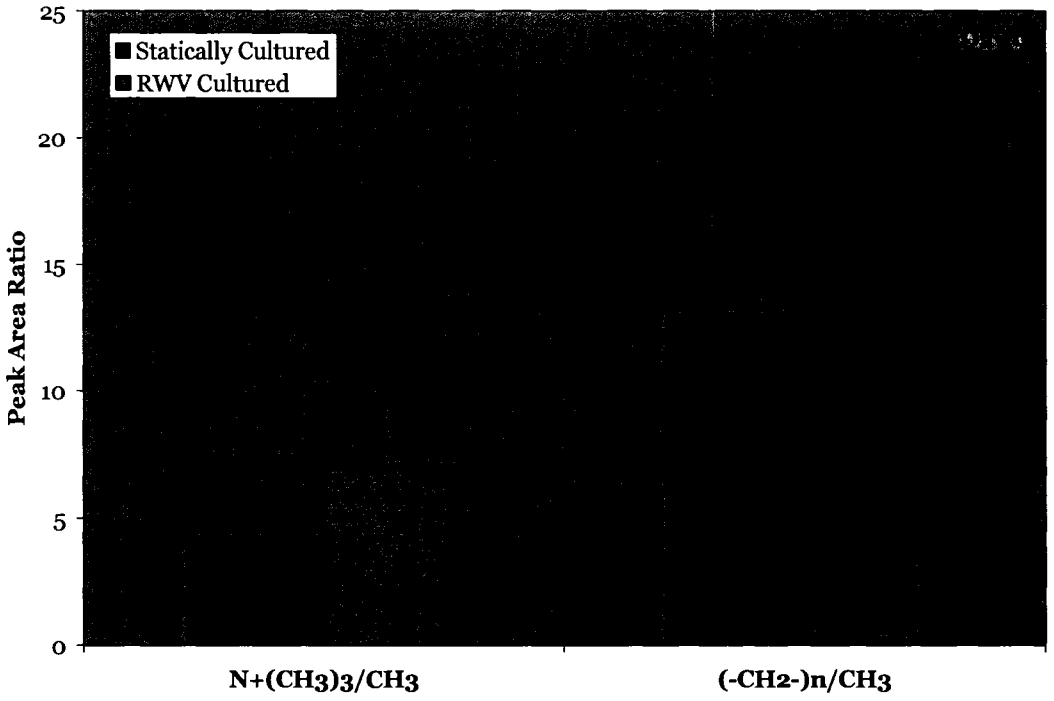

Figure 3-6: Peak area ratios for cells cultured for 9 days under static and low shear conditions. [$N^{+}(CH_3)_3/CH_3$, n = 3, $p<0.001$; $(-CH_2-)n/CH_3$, n = 3, $0.001<p>0.01$]. The error bars represent the standard deviation of the 3 experimental trials.

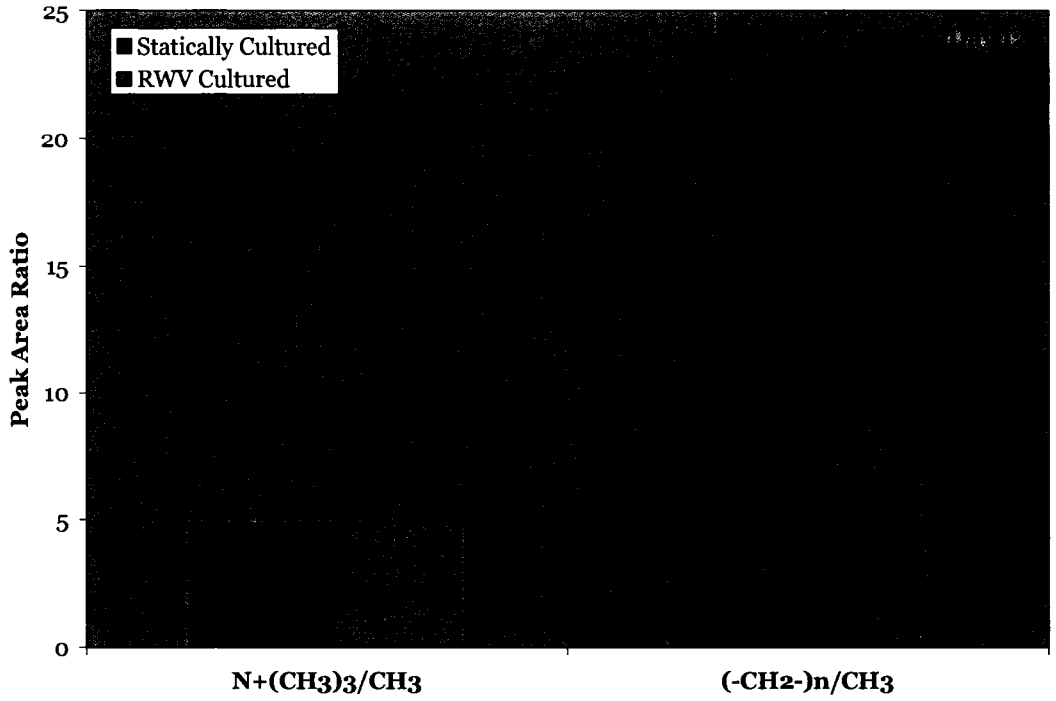

Figure 3-7: Peak area ratios for cells cultured for 12 days under static and low shear conditions. [$N^{+}(CH_3)_3/CH_3$, n = 3, $p<0.001$; $(-CH_2-)n/CH_3$, n = 3, $0.001<p>0.01$]. The error bars represent the standard deviation of the 3 experimental trials.

In order to compare the two sets of experiments we will look at the spectra obtained following 12 days in culture. Recall, in the first set of experiments cells were cultured statically and in a low shear environment for 12 days. In the second set of experiments the choline to methyl ratio remains largely unchanged for cells cultured statically and in a low shear environment (Figure 3.7). There appears to be a minimal increase in choline, however, this increase is within the experimental uncertainty and not statistically significant. Results from the first set of experiments (Figure 3.3) show the choline to methyl peak area ratio appears to increase following 12 days of culture in the RWV, as compared to statically cultured cells. However, there is a significant amount of peak overlap ("noise") in the spectra obtained in the first set of experiments that may lead to the difference between the two results. For cells cultured in a low shear environment for 12 days there is a marked increase in the methylene to methyl peak area ratio compared with cells cultured statically (Figure 3.7). This observation in Figure 3.7 – an increase in methylene to methyl peak area ratio for RWV cultured cells – is in agreement with the first set of experiments (Figure 3.3).

We will now discuss the temporal evolution of Jurkat cells cultured under static and low shear conditions. The temporal evolution of the methylene and choline to methyl peak intensities is best seen in Figures 3.8 and 3.9, respectively. Figures 3.8 and 3.9 are a time series representation of the results shown in Figures 3.5 – 3.7. Following 6, 9 and 12 days of culture, there does not appear to be statistically significant changes in the choline to methyl peak area ratios for statically and RWV cultured cells. When examining the same time periods for the methylene to methyl peak ratio, there appears to be a decrease with time for statically cultured cells, while the same ratio for RWV

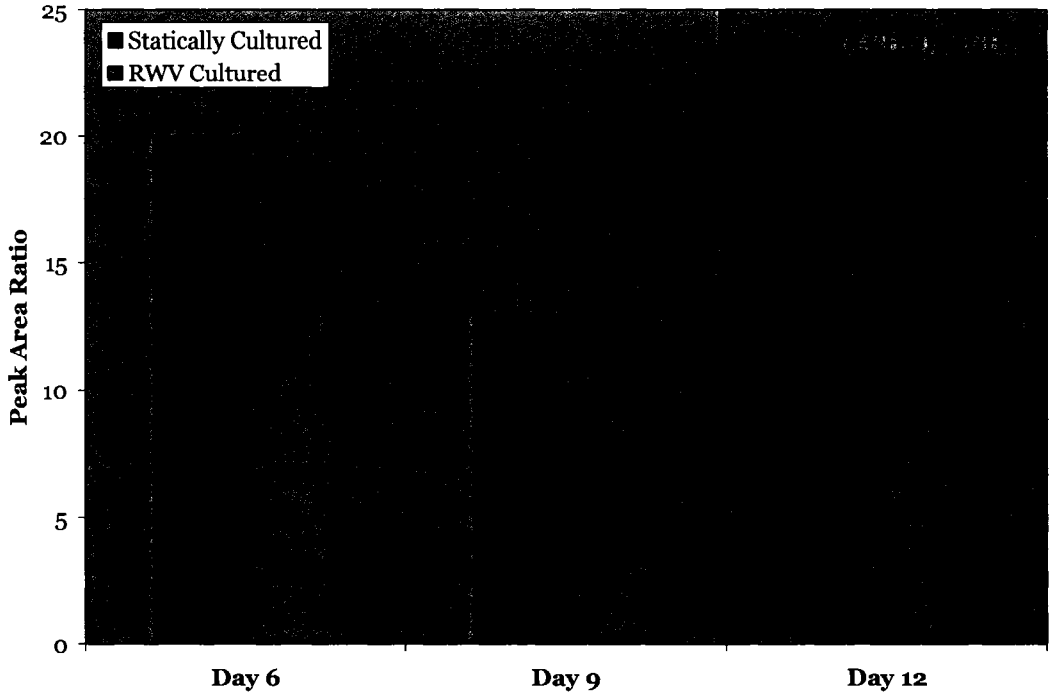

Figure 3-8: Temporal evolution of methylene to methyl peak area ratios for cells cultured under static and low shear conditions.
The error bars represent the standard deviation of the 3 experimental trials.

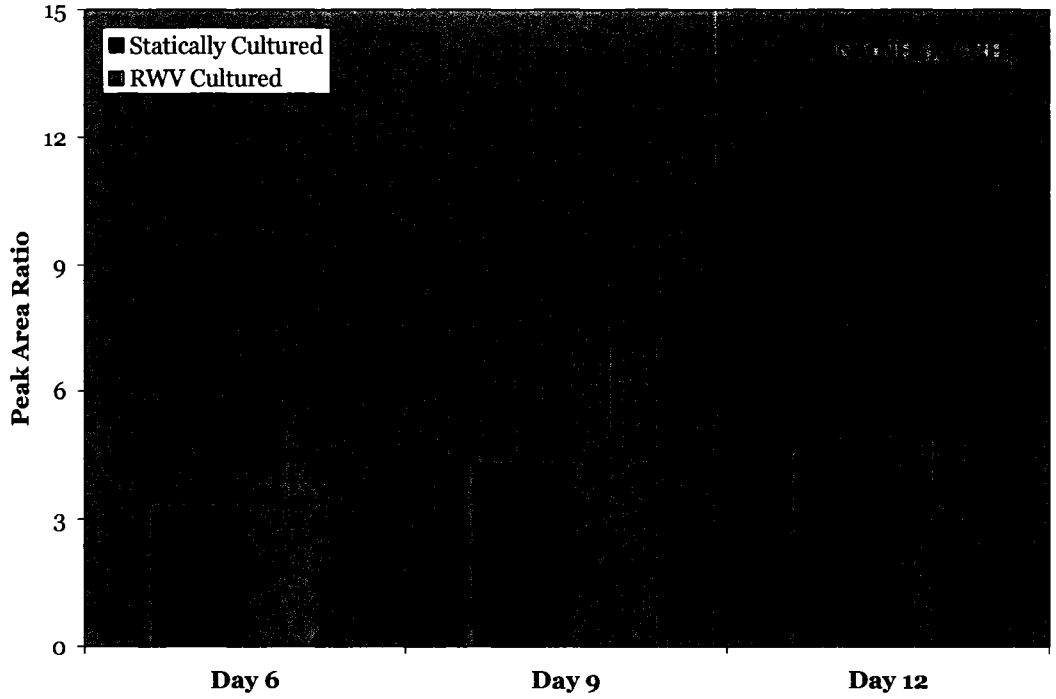

Figure 3-9: Temporal evolution of choline to methyl peak area ratios for cells cultured under static and low shear conditions.
The error bars represent the standard deviation of the 3 experimental trials.

cultured cells appears to be going through a minimum at 9 days. These results clearly show that the choline to methyl peak area ratio remains largely unchanged as a function of time and independent of the method of cell culture. In contrast, the methylene to methyl peak area ratio appears to have a time dependency and is affected by the method of culture.

The methylene to methyl time dependency observed in Figure 3.8 has been seen in Jurkat cells upon exposure to doxorubicin previously [87]. Since the increase of methylene to methyl peak area ratio has been shown to correlate with apoptosis (discussed previously in this chapter), we tested the cell viability following cell culture and NMR analysis. Cell viability was obtained by microscopically examining a portion of the cells with a Trypan Blue exclusion test. In the second set of experiments, cell viability never changed by more than 10% at any point throughout the experimental procedure. In the first set of experiments, cell viability never changed by more than 15%. While we cannot completely rule out the possibility that cell death (apoptosis) contributing to differences in spectra, it is not expected to be significant. The increase (change) in methylene to methyl peak ratio has been associated with a loss of cytoskeletal architecture. It is possible that the loss of cytoskeletal architecture is partly responsible for changes in lipid expression, and that this loss of cytoskeletal structure may allow for increased mobility of the plasma membrane lipids.

Another important observation to consider is that temporal evolution of the methylene to methyl peak ratios are not the same for static and RWV cultured cells (Figure 3.8). These differences are an indication that the culture conditions (i.e., a low shear environment) lead to differences in lipid metabolism, and perhaps membrane

fluidity. These differences in lipid metabolism may explain the observed differences in cell motility between cells cultured statically and in a low shear environment.

4. CONCLUSIONS AND FUTURE WORK

Experiments performed during spaceflight and in ground based studies with RWV have shown dramatic effects on the migratory behavior of lymphocytes. Two ways that mechanical forces may affect cell function are by altering cell-substrate contacts and by direct sensing by the cell of the mechanical force, possibly by a change in cell shape. Research performed in our laboratory indicates that culturing lymphocytes under low shear conditions (in rotating wall vessels) leads to an increase in cell motility and altered cell morphology. ^{1}H-NMR was used to elucidate structural changes in the cytoskeleton - indicated by an increase in lipid visibility - of Jurkat cells cultured in a low shear environment. Ideas for future work to extend and strengthen the results presented in this thesis are discussed.

4.1. Low Sheer Cell Culture Environment

In Chapter 2, we investigated how mechanical forces applied to lymphocytes in a suspension culture effect lymphocyte adhesion and migration after removal from culture. To achieve this, we cultured cells in a rotating wall vessel (RWV) and compared their behavior to statically cultured cells. We found that RWV culture significantly increased the speed of Jurkat cell migration on fibronectin coated surfaces, in agreement with previous studies [75].

The mechanism of how lymphocytes modulate their migratory behavior in response to mechanical forces remains unknown. Cells are thought to sense mechanical

forces through change in cell shape. However, how cells change shape under mechanical stress is poorly understood, especially cells cultured in the RWV. Recent theories suggest that cell shape is modulated through the cytoskeleton arrangements [61]. Mechanical forces affect the balance of forces within on the cytoskeleton, ultimately resulting in shape changes. By understanding how cells change shape under mechanical stresses, the link between cytoskeletal rearrangement and the biochemical response to mechanical forces may be elucidated.

4.2. ^{1}H-NMR Analysis of Lymphocytes Cultured in a Low Sheer Environment

The presence of mobile neutral lipids in the spectra of cells grown under low shear conditions suggests that the cells undergo a change in cell membrane composition and structure. This observation is supported by an increase in cell spreading resulting from low shear culture [74] and is in line with the increased cholesterol content shown by others [51] to be associated with increased membrane fluidity. Furthermore, other researchers [40] have observed that cancer cells with increased cholesterol content exhibit similar spectra to those obtained in the first set of experiments from cells cultured in a low shear environment. This increased cholesterol content resulting in increased membrane fluidity would be in agreement with our first set of experimental results of increased cell motility due to RWV culture. It should be noted; however, that in the second set of experiments the same increase in choline to methyl ratio was not observed. As mentioned previously, these differences may be explained by the peak overlap ("noise") in the first set of experiments.

While we cannot completely explain the differences between the two sets of experiments, there are similarities that demonstrate a significant difference in lipid metabolism between cells cultured statically and in a low shear environment. It is important to note the observed differences in lipid behavior of cells cultured under different conditions may implicate differences in cell motility. Moreover, the increase in the methylene to methyl peak area ratio following 12 days of culture, in both sets of experiments, is quite significant with respect to cell motility. Several studies have shown that an increase in the methylene to methyl peak ratio has been shown to be associated with altered membrane structure. This altered membrane structure, or loss of cytoskeletal structure, may allow for increased mobility of plasma membrane lipids. Also in support of our results, it has been reported is that there may be a time dependence on the degree of plasma membrane mobility. The time-course experimental results presented here clearly indicate a temporal evolution of the methylene to methyl peak area ratio. These results demonstrate that a ^{1}H-NMR spectrum can provide useful qualitative information about changes in lymphocyte cell metabolism and membrane fluidity.

4.3. Future Work

Analysis has shown that within a period of time the cells in the RWV will contact the outer wall due to centrifugal forces. We did not observe cells sticking to the wall of the RWV; however constant cell-wall collisions may affect the cells in an unpredictable manner. Better understanding the dynamics of cells cultured in the RWV would be helpful in understanding the effect of low shear forces on cells in culture.

Cells are thought to sense mechanical forces through change in cell shape. However, how cells change shape under mechanical stress is poorly understood, especially cells cultured in the RWV. Our laboratory [74] has shown that RWV culture leads to changes in cell shape. Altered mechanical forces, represented by a low shear environment in our experiments, affect the balance of forces within on the cytoskeleton, ultimately resulting in shape changes. Using mathematical modeling, the change in shape of cells cultured in the RWV can be estimated. By understanding how cells change shape under mechanical stresses, the link between cytoskeletal rearrangement and the biochemical response to mechanical forces can be elucidated.

Further studies should be carried out to determine the cellular mechanism concerning how the cells modulate their migratory behavior after culture in the RWV. While the ^{1}H-NMR experiments presented here did provide some insight into the relationship between lipid metabolism and cell motility, there is still much to be learned. The results shown here, while enlightening, are only qualitative. Designing a set of quantitative experiments could lead to further discoveries about the effect of an altered mechanical environment on cell shape and hence, cell motility.

5. REFERENCES

1. Kuby J. Immunology. 1992.

2. Springer T. Traffic Signals on Endothelium for Lymphocyte Recirculation and Leukocyte Emigration. Annu Rev Physiol 1995; 57: 827-872.

3. Springer T. Traffic Signals for Lymphocyte Recirculation and Leukocyte Emigration: The Multistep Paradigm. Cell 1994; 76: 301-314.

4. Picker L, Butcher E. Physiological and Molecular Mechanisms of Lymphocyte Homing. Annu Rev Immunol 1992; 10: 561-591.

5. Rouslahti E. Integrins as Signaling Molecules and Targets for Tumor Therapy. Kidney International 1997; 51: 1413-1417.

6. Defilippi P, Gismondi A, Santoni A, Tarone G. Signal Transduction by Integrins. Chapman & Hall, 1997.

7. Seig D, Ilic D, Jones K, Damsky C, Hunter T, Sclaepfer D. Pyk2 and Src-Family Protein Tyrosine Kinases Compensate for the Loss of FAK in Fibronectin-Stimulated Signaling Events but Pyk2 does not Fully Function to Enhance FAK-Cell Migration. EMBO J 1998; 17: 5933-5947.

8. Maguire J, Danahey K, Burkly L, van Seventer G. T Cell Receptor- and the Beta1 Integrin-Mediated Signals Synergize to Induce Tyrosine Phosphorylation of Focal Adhesion Kinase in Human T Cells. J Exp Med 1995; 182: 2079-2090.

9. Dekker L, Parker P. in *Protein Kinase C* (eds. Parker, P & Dekker, L) (1997).

10. Newton A. in *Protein Kinase C* (eds. Dekker, L & Parker, P) (1997).

11. Entschladen F, Niggemann B, Zanker KS, Friedl P. Differential Requirement of Protein Tyrosine Kinases and Protein Kinase C in the Regulation of T Cell Locomotion in Three-Dimensional Collagen Matricies. Journal of Immunology 1997; 159: 3203-3210.

12. Southern C, Wilkinson P, Thorp K, Henderson L, Nemec M, Matthews N. Inhibition of Protein Kinase C Results in a Switch from a Non-Motile Phenotype in Diverse Human Lymphocyte Populations. Immunology 1995; 84: 326-332.

13. Taub D, Key M, Clark D, Turcovski-Corrales S. Chemotaxis of T Lymphocytes on Extracellular Matrix Proteins: Analysis of the in vitro Method to Quantitate Chemotaxis of Human T Cells. J of Immunological Methods 1995; 184: 187-198.

14. Nikolai G, Niggeman B, Werner M, Zanker K, Freidl P. Direct and Rapid Induction of Migration in Human CD4 T Lymphocytes Within Three-Dimensional Collagen Matricies Mediated by Signalling Via CD3 and/or CD2. Immunology 1998; 95: 62-68.

15. Kato K, Mohri H, Tamura T, Okubo T. A Synthetic Peptide, FN-C/H-V from the C-terminal Heparin-Binding Domain of Fibronectin Promotes Adhesion of PMA Stimulated U937 Cells. Biochem Biophys Res Comm 1997; 239: 205-211.

16. Wilkins J, Stupack D, Stewart S, Caixia S. Beta-1 Integrin-mediated Lymphocyte Adherence to Extracellular Matrix is Enhanced by Phorbol Ester Treatement. Eur J Immunol 1991; 21: 517-522.

17. Cogoli A. Space Flight and the Immune System. Vaccine 1993; 11: 497-503.

18. Brown D. in *Clinical Aspects of Immunology, 4th ed.* (eds. Lachmann, P & Peters, D) (Blackwell Scientific Publications, Boston, 1982).

19. Taylor G, Janney R. In vivo Testing Confirms a Blunting of the Human Cell-Mediated Immune Mechanism During Spaceflight. Journal of Leukocyte Biology 1992; 51: 129-132.

20. Gmunder F, Konstantinova I, Cogoli A, Lesnyak A, Bogomolov W, Grachov A. Cellular Immunity in Cosmonauts During Long Duration Spaceflight on Board the Orbital MIR Station. Aviat Space Environ Med 1994; 65: 419-423.

21. Cogoli A, Bechler B, Muller O, Hunzinger E. in *Biorack on Spacelab D1. ESA SP-1091.* (eds. Longdon, N & David, V) (ESA, Paris, 1988).

22. Taylor G, Dardano J. Human Cellular Immune Responsiveness Following Space Flight. Aviat Space Environ Med 1983; 54: S55-S59.

23. Taylor G, Neale L, Dardano J. Immunological Analyses of US Space Shuttle Crew Members. Aviat Space Environ Med 1986; 57: 213-217.

24. Kimzey S. in *Biomedical Results from Skylab* (eds. Johnson, R & Dietlein, L) 249-282 (NASA, 1977).

25. Kimzey S, Fischer C, Johnson P, Ritzmann S, Mengel C. in *Biomedical Results of Apollo* 197-226 (NASA, 1975).

26. Guseva Y, Tashpulatov R. Effect of Flights Differing in Duration on Protein Consumption in Cosmonauts Blood. Space Biol Aerospace Med 1980; 14: 15-20.

27. Guseva Y, Tashpulatov R. Effect of 49-day Space Flight on Parameters of Immunological Reactivity and Protein Consumption of Blood in the Crew of Salyut 5. Space Biol Aerospace Med 1979; 13: 1-7.

28. Sonnenfeld G, Mandel A, Konstantinova I, Taylor G, Berry W, Wellhausen S, Lesnyak A, Fuchs B. Effects of Spaceflight on Levels and Activity of Immune Cells. Aviat Space Environ Med 1990; 61: 648-653.

29. Cogoli A, Tschopp A, Fuchs-Bislin P. Cell Sensitivity to Gravity. Nature 1984; 225: 228-230.

30. Limouse M, Manie S, Konstantinova I, Ferrua B, Schaffar L. Inhibition of Phorbol Ester-Induced Activation in Microgravity. Exp Cell Res 1991; 197: 82-86.

31. Pippia P, Sciola L, Cogoli-Greuter M, Meloni M, Spano A, Cogoli A. Activation Signals of T Lymphocytes in Microgravity. Journal of Biotechnology 1996; 47: 215-222.

32. Stout M, Watenpaugh D, Breit G, Hargens A. Simulated Microgravity Increased Cutaneous Blood Flow in the Head and Leg of Humans. Aviat Space Environ Med 1995; 66: 872-875.

33. Gabrielson A, Norsk P, Videbaek R, Henriksen O. Effect of Microgravity on Forearm Subcutaneous Vascular Resistence in Humans. J Appl Physiol 1995; 79: 434-438.

34. Mcgovern, K., *et al.*, Gel-entrapment of perfluorocarbon: a fluorine-19 NMR spectroscopic method for monitoring oxygen concentration in cell perfusion systems. *Magn Reson Med*, 1993. 29: p. 196-204.

35. Callies, R., M. Jackson, and K. Brindle, Measurements of the growth and distribution of mammalian cells in a hollow-fiber bioreactor using nuclear magnetic resonance imaging. *Biotechnology*, 1994. 12: p. 75-78.

36. Potter, K., *et al.*, Cartilage formation in a hollow fiber bioreactor studied by proton magnetic resonance imaging. *Matrix Biology*, 1998. 17: p. 513-523.

37. Artemov, D., *et al.*, Dynamics of prostate cancer cell invasion studied in vitro by NMR microscopy. *Magn Reson Med*, 1999. 42: p. 277-282.

38. Sieuwerts, A., G. Klijn, and J. Foekens, Assessment of the invasion potential of human gynecological tumor cell lines with the in vitro Boyden chamber essay:

influence of the ability of cells to migrate through the filter membrane. *Clin Exp Metastasis*, 1997. 15: p. 53-62.

39. Rosi, A., *et al.*, H-MRS Lipid Signal Modulation and Morphological and Ultrastructural Changes Related to Tumor Cell Proliferation. *Mag. Res. Med.*, 1999. 42: p. 248-257.

40. Mountford, C., *et al.*, High resolution proton NMR analysis of metastic cancer cells. *Science*, 1984. 226: p. 1415-1418.

41. Lean, C., *et al.*, Cell surface fucosylation and magnetic resonance spectroscopy characterization of human malignant colorectal cells. *Biochemistry*, 1992. 31: p. 11095-11105.

42. Luciani, A., *et al.*, Interaction with HIV-1 with susceptible lymphoblastoid cells. *FEBS Lett*, 1991. 285: p. 11-16.

43. Santini, M., *et al.*, Localized and transient changes in plasma membrane fluidity during in vitro myoblast fusion: An ^{1}H-NMR Study. *Physiol Chem Phys & Med NMR*, 1992. 24: p. 89-96.

44. Dingley, A., N. King, and G. King, An NMR investigation of the changes in plasma membrane triglyceride and phospholipid precursors during the activation of T lymphocytes. *Biochemistry*, 1992. 31(37): p. 9098-9106.

45. May, G., K. Sztelma, and T. Sorrell, The presence of cytoplasmic lipid droplets is not sufficient to account for neutral lipid signals in the ^{1}H-MR spectra of neutrophils. *Magn Res Med*, 1994. 31: p. 212-217.

46. Holmes, K., *et al.*, Development of the "activated" high resolution ^{1}H MR spectrum in murine T cells and B cells occurs in G1 phase of the cells cycle. *Magn Res Med*, 1990. 16: p. 1-8.

47. Russel, P., *et al.*, Proton magnetic resonance and human thyroidneoplasia I: Discrimination between benign and malignant neoplasms. *Am J Med*, 1994. 96: p. 383-388.

48. Mountford, C., *et al.*, *J Biochem Biophys Methods*, 1984. 9: p. 323-330.

49. Holmes, K., *et al.*, *Magn Reson Med Biol*, 1988. 1: p. 75-79.

50. King, N., M. Ward, and K. Holmes, *FEBS Lett*, 1991. 287: p. 97-101.

51. Finegold L., et al (1991) "Cholesterol-multilipid interactions in bilayers." Chem Phys Lipids, 58(1-2):169-73.

52. Rooney, MW; Lange, Y and Kauffman, JW (1984) "Acyl chain organization and protein secondary structure in cholesterol-modified erythrocyte membranes." J Biol Chem 259 (13): 8281-5.

53. Rintoul, DA; Chou, SM; Silbert, DF (1979) "Physical characterization of sterol-depleted LM-cell plasma membranes." J Biol Chem 254 (20): 100707.

54. Sankaram, MB and Thompson, TE (1990) "Modulation of phospholipid acyl chain order by cholesterol. A solid-state 2H nuclear magnetic resonance study." Biochemistry 29 (47):10676-84

55. Okuyama M, Ohta Y, Kambayashi J, Monden M. Fluid Shear Stress Induces Actin Polymerization in Human Neutrophils. Journal of Cellular Biochemistry 1996; 63: 432-441.

56. Neelamengham S, Taylor A, Burns A, Smith C, Simon S. Hydrodynamic Shear Shows Distinct Roles for LFA-1 and Mac-1 in Neutrophil Adhesion in Intercellular Adheion Molecule-1. Blood 1998; 92: 1626-1638.

57. Simon S, Neelamengham S, Taylor A, Smith C. The Multistep Process of Homotypic Neutrophil Aggregation: A Review of the Molecules and Effects of Hydrodynamics. Cell Adhes Commun 1998; 6: 263-276.

58. Berlin C, Bargatze R, Campbell J, Andrian Uv, Szabo M, Hasslen S, Nelson R, Berg E, Erlandsen S, Butcher E. a4 Integrins Mediate Lymphocyte Attachmnt and Rolling Under Physiologic Flow. Cell 1995; 80: 413-422.

59. Schwarz R, Goodwin T, Wolf D. Cell Culture For Three-Dimensional Modeling in Rotating-Wall Vessels: An Application of Simulated Microgravity. J Tiss Cult Meth 1992; 14: 51-58.

60. Duray P, Hatfill S, Pellis N. Tissue Culture in Microgravity. in 1996 .

61. Prewett T, Goodwin T, Spaulding G. Three-Dimensional Modeling of T-2 Human Bladder Carcinoma Cell Line: A New Simulated Microgravity Culture Vessel. J Tiss Cult Meth 1993; 15: 29-36.

62. Hoson T, Kamisaka S, Buchen B, Sievers A, Yamashita M, Masuda Y. Possible Use of a 3-D Clinostat to Analyze Plant Growth Processes Under Microgravity Conditions. Adv Space Res 1996; 17: 47-53.

63. Duke P, Daane E, Montufar-Solis D. Studies of Chondrogenesis in Rotating Systems. J Cell Biochem 1993; 51: 274-282.

64. Freed L, Vunjak-Novakovic G, Langer R. Cultivation of Cell-Polymer Cartilage Implants in Bioreactors. J Cell Biochem 1993; 51: 257-264.

65. Granet C, Laroche N, Vico L, Alexandre C, Lafage-Proust M. Rotating-Wall Vessels, Promising Bioreactors for Osteoblastic Cell Culture: Comparison with Other 3D Conditions. Med Biol Eng Comput 1998; 36: 513-519.

66. Klement B, Spooner B. Utilization of Microgravity Bioreactors for Differentiation of Mammalian Skeletal Tissue. J Cell Biochem 1993; 51: 252-256.

67. Akins R, Schroedl N, Gonda S, Hartzell C. Neonatal Rat Heart Cells Cultured in Simulated Microgravity. in 1991 .

68. Margolis L, Hatfill S, Chuaqui R, Vocke C, Emmert-Buck M, Linehan W, Duray P. Long Term Organ Culture of Human Prostate Tissue in a NASA-Designed Rotating Wall Bioreactor. J Urol 1999; 161: 290-297.

69. Clejan S, O'Connor K, Cowger N, Cheles M, Haque S, Primavera A. Effects of Simulated Microgravity on DU 145 Human Prostate Carcinoma Cells. Biotechnology and Bioengineering 1996; 50: 587-597.

70. Margolis L, Hatfill S, Chuaqui R, Vocke C, Emmert-Buck M, Linehan W, Duray P. Long Term Organ Culture of Human Prostate Tissue in a NASA-Designed Rotating Wall Bioreactor. J Urol 1999; 161: 290-297.

71. Becker J, Prewett T, Spaulding G, Goodwin T. Three-Dimensional Growth ad Differentiation of Ovarian Tumor Cell Line in High Aspect Rotating-Wall Vessel: Morphologic and Embryologic Considerations. J Cell Biochem 1993; 51: 283-289.

72. Margolis L, Fitzgerald W, Glushakova S, Hatfill S, Amichay N, Baibakov B, Zimmerberg J. Lympohcyte Trafficking and HIV Infection of Human Lymphoid Tissue in a Rotating Wall Vessel Bioreactor. AIDS Res Hum Retroviruses 1997; 13: 1411-1420.

73. Long J, Pierson S, Hughes J. Rhinovirus Replication in HeLa Cells Cultured Under Conditions of Simulated Microgravity. Aviat Space Environ Med 1998; 69: 851-856.

74. Bergman, A. (2000). The effects of mechanical forces on lymphocyte adhesion and migration. Chemical Engineering. Houston, Rice University: 178.

75. Bergman, A. and K. Zygourakis (1999). "Migration of lymphocytes on fibronectin coated surfaces: temporal avolution of migratory parameters." Biomaterials 000:

76. Gao, H., P. S. Ayyaswamy, and P. Ducheyne. 1997. Dynamics of a microcarrier particle in the simulated microgravity environment of a rotating wall vessel. Microgravity Sci. Technol. 10:154-165

77. Xie, Xueying, "Modeling Viscoelastic Free Surface and Interfacial Flows, with Applications to the Deformation of Droplets and Blood Cells," Doctoral Dissertation, Rice University, Houston, TX (2006).

78. Munn L, Glacken M, McIntyre B, Zygourakis K. Analysis of lymphocyte Aggragation Using Digital Image Analysis. J Immunol Meth 1993; 166: 11-25.

79. Munn L. The Application of Digital Image Analysis Techniques to Studies of Lymphocyte Function. Ph.D. thesis in Chemical Engineering, Rice University 1993.

80. Lee Y. Computer-Assisted Analysis of Endothelial Cell Migration and Proliferation. Ph.D. thesis in Chemical Engineering, Rice University 1995.

81. Freshney R. Animal Cell Culture. Washington, D.C.: IRL Press, 1986.

82. Stokes CL, Lauffenburger DA, Williams SK. Migration of individual microvessel endothelial cells: stochastic model and parameter measurement. J Cell Sci 1991; 99: 419-430.

83. DiMilla PA, Quinn JA, Albelda SM,Lauffenburger DA. Measurement of Individual Cell Migration Parameters for HUman Tissue Cells. AIChE Journal 1992; 38: 1092-1104.

84. Goodman S, Risse G, von der Mark K. The E8 Subfragment of Laminin Promotes Locomotion of Myoblasts Over Extracellular Matrix. J Cell Biol 1989; 109: 799-809.

85. Mannechez, A, et al (2005) "Proton NMR visible mobile lipid signals in sensitive and multi drug-resistant K562 cells are modulated by rafts" Cancer Cell Intl 5:2.

86. Di Vito, M., Lenti, L, Knijn, A., Iorio, E. D'Agostino, F., Molinari, A., Calcabrini, A., Stringaro, A., Meschini, S., Arancia, G., Bozzi, A., Strom, R. and Podo, F. (2001). "^{1}H NMR-visible mobile lipid domains correlate the cytoplasmic lipid

bodies in apoptotic T-lymphoblastoid cells." Biochimica et Biophysica Acta 1530: 47-66.

87. Blankenberg, F., P. Katsikis, et al. (1997). "Quantitative Analysis of Apoptotic Cell Death Using Proton Nuclear Magnetic Resonance Spectroscopy." Blood 89(May 15): 3778-3786.

88. Holmes, K., C. Lean, et al. (1990). "Development of the "activated" high resolution ^{1}H MR spectrum in murine T cells and B cells occurs in G1 phase of the cells cycle." Magn Res Med 16: 1-8.

89. Pollack, S.R., Meaney, D.F., Levine, E.M., Litt, M., Johnston, E.D., 2000. Numerical model and experimental validation of microcarrier motion in a rotating bioreactor. Tiss. Eng. 6 (5), 519–530.

90. Nauman EA, Ott CM, Sander E, Tucker DL, Pierson D, Wilson JW, Nickerson CA. A Novel Quantitative Biosystem to Model Physiological Fluid Shear Stress on Cells. Appl Environ Microbiol 73: 699-705, 2006.

91. Botchwey EA, Pollack SR, El-Amin S, Levine EM, Tuan RS and Laurencin CT: Human Osteoblast-Like Cells in Three-Dimensional Culture with Fluid Flow. Biorheology 40: 299-306, 2003.

92. Ju Z, Liu T, Ma X, Cui Z. Numerical simulation of microcarrier motion in a rotating wall vessel bioreactor. Biomed Environ Sci 19: 163-168, 2006.

93. Goodwin TJ, Prewett TL, Wolf DA, Spaulding GF, Reduced shear stress: a major component in the ability of mammalian tissues to form three-dimensional assemblies in simulated microgravity. Cell Biochem.51(3):301-11, 1993.

94. Westerhof, Niko. Snapshots of Hemodynamics, Springer 2004.